Astron. Astrophys. 169, 95–110 (1986)

ASTRONOMY AND ASTROPHYSICS

Linear oscillations of isotropic stellar systems

III. A classification of non-radial modes*

Y. Sobouti

[1] Physics Department and Biruni Observatory, Shiraz University, Shiraz, Iran
[2] Astronomy and Astrophysics Center, The University of Chicago, Chicago, USA

Received October 10, 1985; accepted March 17, 1986

Summary. In an expansion scheme in velocity space, the first order perturbations of a stellar system bear close resemblance to those of a fluid. This feature is exploited to study the structure of the Hilbert space of the linear perturbations of a stellar system, to provide a classification for the modes, and to provide the necessary ansatz for variational calculations. The first order non-radial modes appear to be trispectral. Some of their general characteristics are pointed out. The eigenfrequencies and the eigenfunctions of radial ($l=0$) and non-radial ($l=1$) modes of polytropes are calculated. The density waves associated with these modes are also reported.

Key words: globular clusters-stellar dynamics: stability, normal modes – density waves

1. Introduction

On separating the linear perturbations of the Boltzmann-Liouville equation into symmetric and antisymmetric components in the velocity space and eliminating the symmetric component, one arrives at Antonov's equation. Various versions of this eigenvalue equation have been used by some investigators to obtain stability criteria for stellar systems. Yet in a span of a quarter of a century that has elapsed not a single solution of Antonov's equation can be found in the astronomical literature.

The question of whether or not collisionless stellar systems possess global modes of oscillations is unsettled. The opinions range from complete denials that "*there are no phase-coherent phenomena such as overall pulsations*" (King, Dynamics of Star Clusters, 1967) to views that there is a continuum of such modes. Toomre's remarks in his 1977 review of Spiral Structure are:

"*...It may be more instructive... to ask why all this laudable global mode calculating has taken so long.*

The reason involves both principle and complexity. For one thing, it has gradually dawned upon most workers that stable self-gravitating disks (especially ones composed of colliosionless stars) may not even possess many discrete normal modes of the sort that one associates with church bells and cepheids."

Kulsrud and Mark (1970) also express a feeling that "*the normal modes of collisionless systems are generally very singular because of resonent-particle effects ... and there is a continuum of such modes...*". On the other hand, Vandervoort (1983) considers rotating axisymmetric galaxies, uses tensor virial equations in their stellar dynamical forms, and calculates discrete modes of oscillation of toroidal-, shear-, and pulsation-types. Similarly, Kalnajs (1977) maintains that purely oscillatory modes can be derived for flat galaxies.

We do not deal with stellar disks here and are unable to comment on Toomre's and Kalnajs' remarks. We do, however, consider idealized spherically symmetric isotropic systems of collisionless particles, and solve the combined Poisson's and Antonov's equation pertaining to them. Within a scheme of variational calculations, and strictly within the realm of the mean-field approximation (which ignores particle individualities) we obtain discrete global modes. The eigenfrequencies of many of these modes lie outside the range of the admissible particle orbital frequencies and leave no room for a debate on particle-wave resonances.

The question of whether or not the linearized Boltzmann-Liouville equation and its normal-mode solutions are of relevance to actual stellar systems or, for that matter, to computer simulated N-body problems is well worth of consideration. The issue is not pursued here, except for one remark. There are systems in which the normal modes do not induce perturbations in the total self-gravitational energy, and there are classes of modes for spherical systems which do not perturb the local gravitational force field. In such cases a particle placed in the smoothed-out system will not be coupled to the modes. No resonances will take place and the modes will maintain their discrete identity. Other considerations in the concluding section makes the notion of particle-wave resonance a less worisome problem.

The question of whether or not there is a continuum of normal modes in addition to the discrete ones will still remain open. For no variational calculation, including the present one, can claim completeness. The author does, however, feel that with a systematic book-keeping in the six-dimensional phase space and with a proper classification scheme a good deal can be learned about the spectrum of modes and many more sequences of discrete modes will emerge before attending to the question of continuum.

In Papers I and II of this series (Sobouti, 1984, 1985) it was proposed to expand the perturbations of the phase space distribution function in velocity space and to carry out integrations over the velocity coordinates. This reduced Antonov's equation to an eigenvalue problem in the three-dimensional configuration space, which contained a series of vector and tensor fields to be

* Contribution No. 13, Biruni Observatory

solved for. The problem in the configuration space, however, could be tackled in successive approximations. Papers I and II contained applications to the radial perturbations of polytropic and of energy truncated distributions. In this paper we elaborate on the first order non-radial modes. At this level, the problem bears a parallelism to the oscillations of fluid masses. The astronomer's knowledge of the latter problem could be profitably employed to track down the modes and even to provide a classification for them.

A summary of the background and the starting formulas are given in Sect. 2. The first order perturbations are characterized by a vector field, $\boldsymbol{\xi}(\boldsymbol{x})$, which belongs to a Hilbert space. The various subspaces of this space and the basis sets spanning them ate discussed in Sects. 3, 4, and 5. The variational method for solving the eigenvalue problem along with the required matrix elements are developed in Sects. 6 and 7. Numerical results and conclusions are given in Sect. 8.

Notation

The reduction of a phase space perturbation in six dimensions has required six expansions. At each stage it has been necessary to introduce appropriate indices to distinguish the expansion components. To keep the notation under control, it has been essential to exercise utmost economy. The expansions are as follows:

i) Antonov's own expansion of a perturbation $\phi(\boldsymbol{x},\boldsymbol{v})$ into symmetric and antisymmetric parts in $\boldsymbol{v}$, ϕ_+, ϕ_-. We have managed for the most part to work only with antisymmetric functions and have dispensed with the subscript $\pm$.

ii) Expansion of an antisymmetric function of $\boldsymbol{v}$ as an antisymmetric power series of $\boldsymbol{v}$, with indices designating the order of the terms in the expansion. In this paper mostly the first order quantities are dealt with, and the order-designating index is suppressed.

iii) Helmholtz expansion of a vector $\boldsymbol{\zeta}(\boldsymbol{x})$ into scaloidal, poloidal, toroidal types with indices s, p, t, respectively.

iv) and v) Spherical harmonic expansions of scalars and vectors with indices (l, m).

vi) Expansion of a scalar $\chi(r)$ in terms of a basis set, $\{\chi_k(r), k=1,2,\ldots\}$, say, with index k to distinguish the set membership.

All indices pertaining to a quantity are written as subscripts, and in the order (i–vi) above. For example, a symbol ζ_{plmk} will designate a vector of poloidal type, of harmonic order (l, m) and of radial number k. In abbreviated forms suppression of indices from right to left will be permitted. For example, ζ_{plm} will denote a poloidal vector of harmonic numbers (l, m) without designating the radial number, ζ_p will stand for a poloidal vector without other specifications, etc.

The greek subscripts and superscripts will denote the three-dimensional (covariant and contravariant) components of vectors.

2. The first order equation for the non-radial perturbations

The main reference for this section is Paper I of this series (Sobouti, 1984). The equation numbers of this paper are quoted by a preceding roman numeral I. Let $F(E)\ H(-E)$ be a step-like distribution function, where E is the energy integral and H is the step function. Only mildly discontinuous distributions will be considered here. These are defined as having $F|dF/dE|^{-1/2}=0$ at $E=0$ (see Eq. [I.6] and the comments thereof). Let $\phi(\boldsymbol{x},\boldsymbol{v},t)=\phi_+ + \phi_-$ be a perturbation on F, with ϕ_+ and ϕ_- being symmetric and antisymmetric in $\boldsymbol{v}$, respectively. Furthermore, make the transformation $\phi_- = |dF/dE|^{1/2} f(\boldsymbol{x},\boldsymbol{v},t)$ where $f(\boldsymbol{x},\boldsymbol{v},t)$ is a new antisymmetric function of $\boldsymbol{v}$. Antonov's equation governing these perturbations are (see Eqs. [I.3] and [I.6])

$$\frac{\partial}{\partial t}\phi_+ + D\phi_- = 0, \tag{1a}$$

$$\frac{\partial^2}{\partial t^2} f + \mathcal{W}1 f + \mathrm{sign}(F_E)\ \mathcal{W}2 f = 0, \tag{1b}$$

where, $F_E = dF/dE$,

$$D = v_\nu \frac{\partial}{\partial x_\nu} - \frac{\partial U}{\partial x_\nu}\frac{\partial}{\partial v_\nu}, \tag{2a}$$

$$\mathcal{W}1 f = -D^2 f, \tag{2b}$$

$$\mathcal{W}2 f = -G|F_E|^{1/2} D \int |F'_E|^{1/2} D' f' |\boldsymbol{x}-\boldsymbol{x}'|^{-1}\, d\tau'. \tag{2c}$$

A prime on a function or on an operator means that the function or the operator in question is to be evaluated at $(\boldsymbol{x}', \boldsymbol{v}')$. An element of the phase space volume is denoted by $d\tau' = d\boldsymbol{x}'\, d\boldsymbol{v}'$. For the standing wave solutions, $f = f(\boldsymbol{x},\boldsymbol{v})\exp(i\omega t)$, Eq. (1b) provides the variational equation

$$\omega^2 = [W1 + \mathrm{sign}(F_E)\ W2]/S, \tag{3}$$

where

$$S = \int f^* f\, d\tau > 0, \tag{4a}$$

$$W1 = \int f^* \mathcal{W}1 f\, d\tau \geqq 0, \tag{4b}$$

$$W2 = \int f^* \mathcal{W}2 f\, d\tau \geqq 0. \tag{4c}$$

A scheme of reduction of Eqs. (3) and (4) into equations in the three-dimensional $\boldsymbol{x}$-space is developed in Paper I (see, in particular, Eq. [I.19a]). Briefly it consists of (a) expanding f as an antisymmetric power series of the vector $\boldsymbol{v}$, (b) substituting the series in Eqs. (3) and (4), and (c) carrying out the integrations over the velocity space. A solution of Eqs. (3) and (4) in successive approximations then becomes feasible. In the first order one assumes

$$f(\boldsymbol{x},\boldsymbol{v}) = \boldsymbol{\xi}(\boldsymbol{x})\cdot\boldsymbol{v}, \qquad v < v_{\mathrm{esc}}, \tag{5}$$

where $\boldsymbol{\xi}(\boldsymbol{x})$ is a vector field to be determined. Let us elaborate on this ansatz. First we note that Eq. (19b) of Paper I, of which equation (5) is the first term, provides an absolutely convergent series for f in powers of $\boldsymbol{v}$. It is a property of absolutely convergent series that there is a number N such that for any $n > N$ the n-th term is less significant than the preceding one. In the case of our expansion there are reasons to believe that this property holds from the beginning. The ratio of successive terms is proportional to $n!/(n+2)! = 1/(n+1)(n+2)$. Secondly, a variational principle underlies Eq. (3). Truncation of the series in any approximation gives a variational expression for Eq. (3) Thus, while Eq. (5) is not expected to satisfy the differential Eq. (16), it is a perfectly legitimate variational ansatz for Eq. (3). The second order accuracy of the calculated eigenfrequencies is guaranteed by the variational principle. More restrictive ansatz, assuming f linear both in $\boldsymbol{x}$ and $\boldsymbol{v}$ can be found in the literature. By means of such ansatz, Vandervoort (1983) reduces the problem to a set of Chandrasekhar-type tensor virial equations.

The linear dependence of f on $\boldsymbol{v}$ in Eq. (5) should not give the impression that heavier weights are assigned to high velocity stars either in perturbed or unperturbed states. (a) Restriction to linear

perturbations, $|f| \ll F$ for all $\boldsymbol{x}$ and $\boldsymbol{v}$, does not allow velocities larger than the velocity of escape. This is in accord with the general belief that escapes from a cluster are unimportant in dynamical time scales. (b) The same restriction imposes severe boundary behavior on $\boldsymbol{\xi}(\boldsymbol{x})$ and forces it to decrease rapidly enough to prevent divergences. A detailed analysis of these boundary conditions is gives in Sect. 4.

As we shall see in Eq. (7), $\boldsymbol{\xi}$ is intimately related to the Lagrangian displacement of a material element of the system in its perturbed state. Explicit expressions for the S-, $W1$-, and $W2$-integrals for this ansatz are (see Eqs. [I.27–29]).

$$S = \int \Phi 2\, \boldsymbol{\xi}^* \cdot \boldsymbol{\xi}\, d\boldsymbol{x} > 0, \tag{6a}$$

$$W1 = \int \Phi 4\, [\partial_\nu \xi^{\mu *} \partial^\nu \xi_\mu + 2\partial_\nu \xi^{\mu *} \partial_\mu \xi^\nu]\, d\boldsymbol{x} + \int \Phi 2\, \partial_{\mu\nu} U \xi^{\mu *} \xi^\nu\, d\boldsymbol{x} \geqq 0, \tag{6b}$$

$$W2 = G \int \boldsymbol{\nabla} \cdot (\Psi \boldsymbol{\xi}^*)\, \boldsymbol{\nabla}' \cdot (\Psi \boldsymbol{\xi}) |\boldsymbol{x} - \boldsymbol{x}'|^{-1}\, d\boldsymbol{x}\, d\boldsymbol{x}' \geqq 0, \tag{6c}$$

where

$$\Phi 2(r) = \frac{4\pi}{15} v_{\mathrm{esc}}^{5/2}, \qquad \Phi 4(r) = \frac{4\pi}{105} v_{\mathrm{esc}}^{7/2}, \tag{7a}$$

$$\Psi(r) = \frac{4\pi}{15} \int_0^{v_{\mathrm{esc}}} |dF/dE|^{1/2} v^4\, dv, \tag{7b}$$

$$v_{\mathrm{esc}}(r) = \text{escape velocity from } r = \sqrt{-2U}, \tag{7c}$$

$$U(r) = \text{the equilibrium gravitational potential, normalized to vanish at the boundary of the system.} \tag{7d}$$

The positive definite character of the S-integral is evident. The positive character of the $W1$- and $W2$-integrals are shown in Paper I, Eqs. (I.8) and (I.9). Furthermore, the eigenvalues ω^2 are real. The eigenfunctions $\boldsymbol{\xi}(\boldsymbol{x})$ exist and belong to a Hilbert space H in which the inner product is $(\boldsymbol{\eta}, \boldsymbol{\zeta}) = \int \Phi 2\, \boldsymbol{\eta}^* \cdot \boldsymbol{\zeta}\, d\boldsymbol{x}$, $\boldsymbol{\eta}$ and $\boldsymbol{\zeta} \in H$. This form of the inner product is dictated by the form of the S-integral. At this stage we observe a close parallelism between the eigenvalue problem of Eqs. (3) and (6) and the eigenvalue problem for the normal modes of an inviscid fluid. For a fluid system one assumes a Lagrangian displacement vector $\boldsymbol{\xi}(\boldsymbol{x})$, and obtains an eigenvalue equation and a variational integral for ω^2 and $\boldsymbol{\xi}$. The important aspect of the parallelism is the vector natur of $\boldsymbol{\xi}$ in both problems and will be exploited extensively here. A lesser aspect of the similarity is that in both cases there is a $W2$-integral which comes from perturbations of the self-gravitation and is identical in both problems. The $W1$-integral, however, is different in the two cases, and causes significant differences between the normal modes of a stellar system and those of a fluid.

One very useful and systematic way of solving Eqs. (3) and (6), that works in fluids, and will also be followed here, is (a) to sort out the main subspaces of H on the basis of physical considerations, (b) to devise appropriate basis sets of vectors to span each subspace, (c) to expand $\boldsymbol{\xi}$ in terms of the basis vectors, (d) to solve the variational Eqs. (3) and (6) for the expansion coefficients, and (e), depending on the size of the projections of $\boldsymbol{\xi}$ on each subspace to assign a *class* to each mode.

Items (a) and (b) are worked out in Sect. 3–5. Computation and classification of the modes [items (c–e)] is carried out in Sects. 6–8. Presentations of these sections are of a somewhat formal nature. To ameliorate the situation a description of the main results is given at this point.

i) Spherical stellar systems may have discrete normal modes of oscillations. Periods of most of the modes are of the order of but shorter than the dynamical time scales.

ii) The modes may be purely radial, $m = 0$, $l = 0$. The corresponding Lagrangian displacement vector is then derivable from a scalar potential (Sect. 8a).

iii) The non-radial modes may possess axial symmetry ($m = 0$) or belong to $m = 1, 2, \ldots$ symmetries.

iv) If $m = 0$ or 1, the modes possess a definite l-symmetry as well. If $m \geqq 2$, however, terms of different l-symmetries get weakly coupled.

v) For a given l and m, it is possible to construct three distinct types of Lagrangian displacements, one derivable mainly from a scalar potential, a second mainly from a toroidal vector potential and a third exclusively from a poloidal vector potential (Sects. 6, and 8b).

vi) Based on their potentials, the modes may be classified as *scaloidal*, *poloidal*-, and *toroidal*-types. The classification is completely analogous to the *p*-, *g*-, and *toroidal*-classification of stellar oscillations.

vii) Associated with each mode is an Eulerian density change which may be considered as standing density waves (Sect. 7 and Figs. 1–10).

3. The subspaces of H

3.1. *A subdivision based on the potentials generating the vector fields*

Let H be a Hilbert space with elements $\boldsymbol{\zeta}(\boldsymbol{x})$, three dimensional vector fields defined over the volume of the stellar system. Let the inner product in H be $(\boldsymbol{\zeta}, \boldsymbol{\zeta}') = \int \Phi 2\, \boldsymbol{\zeta}^* \cdot \boldsymbol{\zeta}'\, d\boldsymbol{x} = \textit{finite}$ and *real*, $\boldsymbol{\zeta}, \boldsymbol{\zeta}' \in H$, where $\Phi 2$ is defined in Eq. (7a). By a modified version of Helmholtz' theorem (Sobouti, 1981, Eq. [7]), $\boldsymbol{\zeta}$ can be expressed in terms of a scalar and a vector potential. Thus

$$\Phi 2\, \boldsymbol{\zeta} = -\Phi 2\, \boldsymbol{\nabla} \chi_{\mathrm{s}} + \boldsymbol{\nabla} \times \boldsymbol{A}, \qquad \boldsymbol{\nabla} \cdot \boldsymbol{A} = 0, \tag{8}$$

where $\chi_{\mathrm{s}}(\boldsymbol{x})$ is a scalar field (the subscript s will be explained shortly), and $\boldsymbol{A}(\boldsymbol{x})$ is a divergence-free vector field. The wisdom of introducing $\Phi 2$ in Eq. (8) will surface when we discuss the orthogonality of the fields. A vector in three dimensions can be chosen in three independent ways. The solenoidal character of $\boldsymbol{A}$, however, limits its choice to two. We shall choose to decompose $\boldsymbol{A}$ into toroidal and poloidal components. Thus, $\boldsymbol{A} = \boldsymbol{\nabla} \times (\hat{\boldsymbol{r}} \chi_{\mathrm{p}}) + \boldsymbol{\nabla} \times \boldsymbol{\nabla} \times (\hat{\boldsymbol{r}} \chi_{\mathrm{t}})$, where $\hat{\boldsymbol{r}}$ is a unit vector along the r-direction, and $\chi_{\mathrm{p}}(\boldsymbol{x})$ and $\chi_{\mathrm{t}}(\boldsymbol{x})$ are two scalar fields. Substituting this in Eq. (8) gives

$$\boldsymbol{\zeta} = \boldsymbol{\zeta}_{\mathrm{s}} + \boldsymbol{\zeta}_{\mathrm{p}} + \boldsymbol{\zeta}_{\mathrm{t}}, \tag{9}$$

where

$$\boldsymbol{\zeta}_{\mathrm{s}} = -\boldsymbol{\nabla} \chi_{\mathrm{s}}, \tag{9a}$$

$$\boldsymbol{\zeta}_{\mathrm{p}} = \boldsymbol{\nabla} \times \boldsymbol{\nabla} \times (\hat{\boldsymbol{r}} \chi_{\mathrm{p}})/\Phi 2, \tag{9b}$$

$$\boldsymbol{\zeta}_{\mathrm{t}} = \boldsymbol{\nabla} \times \boldsymbol{\nabla} \times \boldsymbol{\nabla} \times (\hat{\boldsymbol{r}} \chi_{\mathrm{t}})/\Phi 2. \tag{9c}$$

We shall borrow a nomenclature from Elsasser (1946). The component $\boldsymbol{\zeta}_{\mathrm{s}}$ will be referred to as the *scaloidal* field and it is derived from a scalar potential. The $\boldsymbol{\zeta}_{\mathrm{p}}$ and $\boldsymbol{\zeta}_{\mathrm{t}}$ will be called *poloidal* and *toroidal* fields, respectively. The subscripts s, p, t accompanying $\boldsymbol{\zeta}$ and χ are to remind this nomenclature. Because of division by $\Phi 2$ the poloidal field of Eq. (9b) is not exactly solenoidal. Its divergence, however, is small. Because of vanishing radial components, however, the toroidal field is exactly solenoidal.

We shall mainly deal with spherically symmetric systems. For future reference the spherical polar components of the various fields are given below,

$$\zeta_s = \left(\partial_r \chi_s,\ -\frac{1}{r}\partial_\theta \chi_s,\ -\frac{1}{r\sin\theta}\partial_\phi \chi_s\right), \tag{10a}$$

$$\zeta_p = \frac{1}{\Phi 2}\left(\frac{1}{r^2} L^2 \chi_p,\ \frac{1}{r}\partial_r\partial_\theta \chi_p,\ \frac{1}{r\sin\theta}\partial_r\partial_\phi \chi_p\right) \tag{10b}$$

$$\zeta_t = \frac{1}{\Phi 2}\left(0,\ \frac{1}{r\sin\theta}\partial_\phi \chi_t,\ -\frac{1}{r}\partial_\theta \chi_t\right), \tag{10c}$$

where

$$L^2 = -\frac{1}{\sin\theta}\partial_\theta(\sin\theta\,\partial_\theta) + \frac{1}{\sin^2\theta}\partial_\phi^2, \tag{10d}$$

and χ_t in Eq. (10c) is now redefined to simplify the form of ζ_t.

An immediate conclusion from Eq. (9) is the subdivision of H into three orthogonal subspaces, H_s, H_p, and H_t, with elements ζ_s, ζ_p, and ζ_t respectively. The orthogonality of H_s and H_p is seen from

$$\int \Phi 2\,\zeta_s^* \cdot \zeta_p\, dx = -\int \nabla\chi_s^* \cdot \nabla\times\nabla\times(\hat{r}\chi_p)\, dx$$
$$= -\int \chi_s^* \nabla\cdot[\nabla\times\nabla\times(\hat{r}\chi_p)]\, dx = 0. \tag{11}$$

The orthogonality of H_s and H_t is verified similarly. The orthogonality of H_p and H_t is easily verified by expressing the inner product (ζ_p, ζ_t) in spherical polar coordinates and carrying out integrations over the polar angles. See Chandrasekhar (1962, Appendix III) for details. The reason for the introduction of $\Phi 2$ in Eqs. (8) and (9) is now clear. It guarantees the orthogonality of H_s and H_p and brings in considerable simplification in numerical computations of the eigenmodes.

Let us point out some of the analogies between the fluid problem and the stellar system case.

Small perturbations of a fluid are conventionally divided into three categories: a) Acoustic- or pressure-type of motions which induce substantial pressure fluctuations. b) Convective- or gravity-type of motions. Their existence depends on two factors, a temperature difference between the moving element and its surroundings, and a gravitational field to pervade the fluid. c) Toroidal motions which are slidings of layers of fluid on equipotential surfaces. Due to sheer free nature of an inviscid fluid, toroidal motions do not cause deviations from equilibrium states. From the mathematical point of view the vector fields associated with the above motions are, indeed, those of Eqs. (9) and (10), the only and the insignificant difference being that the density ϱ of the fluid replaces $\Phi 2$. These mathematical properties are spelled out in detail by Sobouti, 1981.

3.2. *Further subdivision based on spherical harmonics*

A spherical harmonic expansion of χ_s, χ_p, and χ_t will result in a corresponding expansion of ζ_s, ζ_p, and ζ_t. Thus,

$$\chi_\alpha(r,\theta,\phi) = \sum_{l,m} \chi_{\alpha l}(r)\ Y_{lm}(\theta,\phi), \tag{12}$$

where α is a generic index denoting s, p, or t. Substituting Eq. (12) in Eqs. (10) gives:

$$\zeta_\alpha = \sum_{l,m} \zeta_{\alpha lm}, \qquad \alpha = \mathrm{s,p,t}, \tag{13}$$

where

$$\zeta_{slm} = \left[-\partial_r \chi_{sl}\, Y_{lm},\ -\frac{1}{r}\chi_{sl}\partial_\theta Y_{lm},\ -\frac{im}{r\sin\theta}\chi_{sl}\, Y_{lm}\right], \tag{13a}$$

$$\zeta_{plm} = \frac{1}{\Phi 2}\left[\frac{l(l+1)}{r^2}\chi_{pl}\, Y_{lm},\ \frac{1}{r}\partial_r\chi_{pl}\partial_\theta Y_{lm},\ \frac{im}{r\sin\theta}\partial_r\chi_{pl}\, Y_{lm}\right], \tag{13b}$$

$$\zeta_{tlm} = \frac{1}{\Phi 2}\left[0,\ \frac{im}{r\sin\theta}\chi_{tl}\, Y_{lm},\ -\frac{1}{r}\chi_{tl}\partial_\theta Y_{lm}\right]. \tag{13c}$$

Any two distinct vectors of Eqs. (13) are mutually orthogonal in H, in the sense that $\int \Phi 2\,\zeta_{\alpha lm}\zeta_{\beta kn}\, dx = 0$, for $(\alpha, l, m) \neq (\beta, k, n)$. A consequence of Eqs. (13) is the further subdivision of any of H_α, $\alpha = \mathrm{s, p, t}$, into smaller orthogonal subspaces $H_{\alpha lm}$ with elements $\zeta_{\alpha lm}$, $\alpha = \mathrm{s, p. t.}$

Before we proceed further the boundary conditions on the elements of H should be clarified.

4. Boundary conditions and analyticity in H

4.1. *Lagrangian displacements*

Associated with the phase space perturbation ϕ_- is a macroscopic velocity field $\boldsymbol{u}(\boldsymbol{x}) = \varrho^{-1}\int \phi_-\, \boldsymbol{v}\, d\boldsymbol{v}$, where ϱ is the equilibrium mass density of the system. In analogy with fluids, a Lagrangian displacement field $\boldsymbol{\eta}(\boldsymbol{x})$ is defined by $\boldsymbol{u} = \dot{\boldsymbol{\eta}}$. Letting $\phi_- = |F_E|^{1/2}\,\boldsymbol{\xi}\cdot\boldsymbol{v}$ [see Eq. (5)] and using Eq. (7b) gives

$$\boldsymbol{\eta} = \frac{i}{\omega}\frac{\Psi}{\varrho}\,\boldsymbol{\xi}. \tag{14}$$

Thus $\boldsymbol{\xi}$ at any position $\boldsymbol{x}$ is proportional to the Lagrangian displacement of a material element of the system, $\boldsymbol{\eta}$. A justification for interpreting $\boldsymbol{\eta}$ as a Lagrangian displacement is provided in Eqs. (15) below, the expressions for the density perturbations. Its main role, however, will be seen shortly when we raise the question of the boundary conditions for $\boldsymbol{\xi}$.

4.2. *Density perturbations*

The Eulerian change in the density is $\delta\varrho = \int \phi_+\, d\boldsymbol{v}$, where ϕ_+ is the symmetric-in-$\boldsymbol{v}$ part of the perturbation in the distribution function. Substituting for ϕ_+ from Eq. (1a) and using Eq. (4) yields

$$\delta\varrho = \frac{i}{\omega}\,\nabla\cdot(\Psi\boldsymbol{\xi}) = -\nabla\cdot(\varrho\boldsymbol{\eta}). \tag{15a}$$

The Lagrangian density change follows from the conventional definition of it,

$$\Delta\varrho = \delta\varrho + \nabla\varrho\cdot\boldsymbol{\eta} = -\varrho\nabla\cdot\boldsymbol{\eta}. \tag{15b}$$

4.3. *Surface boundary conditions*

Let n denote an effective polytropic index of the equilibrium state near the surface. (In principle, one can do without this notion. We are adopting it merely to economize in writing). Some of the attributes of the equilibrium structure behave as follows. As r tends to its surface value R:

$$U \to r - R \to 0, \tag{16a}$$

$$\varrho \to |U|^n, \tag{16b}$$

$$\Phi j \to |U|^{(2j+1)/2}, \qquad j = 0, 2, 4, \ldots, \tag{16c}$$

$$\Psi \to |U|^{(2n+5)/4}, \qquad \text{see Eq. (I.42b)} \tag{16d}$$

$$\frac{\Psi}{\varrho \Phi 2} \to |U|^{-(2n+5)/4}. \tag{16e}$$

As the surface boundary condition, all components of the Lagrangian displacement vector, η, will be required to remain finite at R. From Eqs. (14), (13), and (16), this leads to

$$\partial_r \chi_{sl} \to \frac{\varrho}{\Psi} \to |r-R|^{(2n-5)/4}, \tag{17a}$$

$$\partial_r \chi_{pl} \to \frac{\varrho \Phi 2}{\Psi} \to |r-R|^{(2n+5)/4}, \tag{17b}$$

$$\partial_r \chi_{tl} \to \frac{\varrho \Phi 2}{\Psi} \to |r-R|^{(2n+5)/4}. \tag{17c}$$

Integrating these in the radial direction near the surface gives

$$\chi_{sl} \to |r-R|^{(2n-1)/4} \to \left.\frac{\varrho U}{\Psi}\right|_R, \tag{18a}$$

$$\chi_{pl} \to |r-R|^{(2n+9)/4} \to \left.\frac{\varrho U \Phi 2}{\Psi}\right|_R, \tag{18b}$$

$$\chi_{tl} \to |r-R|^{(2n+5)/4} \to \left.\frac{\varrho \Phi 2}{\Psi}\right|_R. \tag{18c}$$

The left hand side of these equations are constructed from the asymptotic behaviors expressed in Eqs. (16), and are for future reference.

In fluids, the boundary conditions are commonly taken to be the finiteness of $\Delta\varrho/\varrho$ (e.g., Cox and Giuli, 1968) and/or continuity of the perturbed potential and its derivatives across the surface (e.g., Ledoux and Walraven, 1958). For the sake of brevity we do not present similar calculations for stellar systems here. It has, however, been verified that these requirements are met by the conditions of Eqs. (18).

4.4. *Analyticity near the center*

Solutions of Eqs. (3) and (6) must be analytic at $r=0$. A straightforward way of selecting such solutions is to go back to the differential equation (I.30) governing ξ, substitute series of the form $r^j(1+r^2+\ldots)$ for the various components of ξ and for the other structural functions appearing there, and find an indicial equation for the exponent j by equating the coefficients of the lowest power of r to zero. This has almost been done, except that instead of Eq. (I.30), new and simpler variational equations were derived from the S-, $W1$-, and $W2$-integrals given in Eqs. (23) below. The results are reported below.

The scalar potential χ_{sl} tends to a solution of Laplace's equation at the center

$$\chi_{sl} \to r^l \to 0. \tag{19a}$$

For χ_{pl} and χ_{tl} one finds

$$\chi_{pl} \to r^{l+1} \to 0, \tag{19b}$$

$$\chi_{tl} \to r^{l+1} \to 0. \tag{19c}$$

With these asymptotic behaviors, $\nabla \cdot \zeta_{sl}$ and $\nabla \cdot \zeta_{pl}$ also tend to r^l near the center. It is remarkable that the Lagrangian displacement of a fluid for pressure and gravity modes, and their divergences exhibit identical behavior. See Sobouti (1977, Eqs. [19] and [24]) and Hurley et al. (1966, Eqs. [30] and [39]). The toroidal vector ξ_{tl} is divergence-free throughout the system. It can neither be compared with those of a spherical inviscid fluid. For similar displacements of such fluids are neutral and there is no equation of motion to rely on. It is, however, comforting to note that the solid body rotations of the system, say $\xi_{t10} = (0, 0, r\sin\theta)$ belonging to $l=1$, $m=0$, are among the motions generated by Eq. (19c).

5. Basis sets for various subspaces of H

The modified Helmholtz decomposition of Eqs. (9) and (10) is unique, orthogonal, and complete, in the sense that any vector $\zeta(x)$ can be uniquely expressed in terms of three mutually orthogonal components ζ_s, ζ_p, and ζ_t. Therefore, the division of H into the orthogonal subspaces H_s, H_p, and H_t is unique. The spherical harmonic decomposition of Eqs. (12) and (13) is also unique, orthogonal, and complete. Therefore, the subdivision of each H_α, $\alpha = s, p, t$, into the corresponding orthogonal subspaces $H_{\alpha lm}$ is unique. To complete the task one has only to provide a basis set for each $H_{\alpha lm}$, $\alpha = s, p, t$. This can be accomplished by divising a set of complete scalars in the interval $(0, R)$ and expanding the potentials $\chi_{\alpha l}(r)$, $\alpha = s, p, t$, in terms of them. We resort to the Stone-Weierstrass theorem:

If A is an algebra of real continuous functions on the compact interval $(0, R)$ which separates points in $(0, R)$, and if A vanishes at no point in $(0, R)$, then the uniform closure B of A consists of all real continuous functions on $(0, R)$.

The set of the even powers of r, $\{r^{2i}, i=0,1,\ldots\}$, in $(0, R)$ is an algebra and satisfies the conditions of the theorem. Thus, any continuous real-valued function on $(0, R)$ can be approximated uniformly as a linear combination of r^{2i}, $i=0,1,\ldots$. By Eqs. (18a) and (19a) the expression $\chi_{sl} r^{-l} \Psi \varrho^{-1} U^{-1}$ is a continuous real-valued function of r in $(0, R)$. Therefore it can be expanded in even powers of r. The same is true of the expression $\chi_{pl} r^{-l-1} \Psi \varrho^{-1} U^{-1} \Phi 2^{-1}$, which follows from Eqs. (18b) and (19b), and of $\chi_{tl} r^{-l-1} \Psi \varrho^{-1} \Phi 2^{-1}$ which follows from Eqs. (18c) and (19c). The long sought basis sets follow immediately:

$$\chi_{slk} = \frac{\varrho U}{\Psi} r^{l+2k}, \qquad k=0,1,2,\ldots, \tag{20a}$$

$$\chi_{plk} = \frac{\varrho U \Phi 2}{\Psi} r^{l+2k+1}, \qquad k=0,1,2,\ldots, \tag{20b}$$

$$\chi_{tlk} = \frac{\varrho \Phi 2}{\Psi} r^{l+2k+1}, \qquad k=0,1,2,\ldots, \tag{20c}$$

where we have added a third subscript k to denote the radial dependence of the χ-scalars. Unlike the expansions of Eqs. (9) and (13), the expansion of Eqs. (20) is not orthogonal. It is, however, complete and provides a simple ansatz for numerical calculations. More details on these basis sets in the context of fluid systems can be found in Dixit et al. (1980).

In summary, the Hilbert space H of the ξ vectors, describing the first order-in-v perturbations of a stellar system, is exactly the same as the Hilbert space of the Lagrangian displacements of a fluid system. Both spaces can be subdivided identically and can have identical basis sets, etc. This does not, however, mean that the eigensolutions of the two problems are identical. One deals with two different operators. Some of the differences will be pointed out in Sect. 6 as we work through the equations of motion, Eqs. (3) and (4). Some more will be discussed in the concluding Sect. 8.

6. Eigensolutions belonging to $m=0$ and ± 1

In the course of this section the following conclusions will gradually emerge.

i) Spherically symmetric perturbations, $l=m=0$, are of scaloidal-type only (see Eqs. [13b] and [13c] for vanishing of ζ_p and ζ_t). They are not coupled to perturbations belonging to other (l, m) values. Therefore, one may speak of spherically symmetric scaloidal radial modes of stellar systems. This property is sheared by fluids.

ii) Perturbations belonging to different m values are not coupled together. Therefore, one may assign a definite m-symmetry to a normal mode of the system. This property is sheared by fluids.

iii) Perturbations belonging to the same m but different l's are, in general, coupled together [exceptions are $m=0$ and ± 1, and will be discussed in (iv)]. The coupling comes about in the following way. A scaloidal and/or poloidal perturbation belonging to a given (m, l) is coupled with a toroidal perturbation belonging to $m, l\pm 1)$, and vice versa. This causes a second order coupling between (m, l) and $m, l\pm 2)$ perturbations of any of the s-, p-, and t-types. Therefore, strictly speaking, one may not assign a definite l-symmetry to a normal mode. The coupling, however, is weak, and one may still do so approximately. Such a coupling does not exist in fluids.

iv) If $m=0$ or ± 1, the coupling between l's discussed in (iii) vanishes. The modes acuire a definite l-symmetry. They are either of purely toroidal-type or of mixed scaloidal-poloidal types. Furthermore, the eigenvalues become independent of $m=0$, or ± 1 and are three-fold degenerate (provided $l\geqq 1$). The fluids have the same characteristics, except that their pure toroidal perturbations are always neutral.

In the remainder of this paper we shall confine the analysis to the simpler modes of $m=0$ and ± 1. Because of coupling of item (iii) above, the cases of higher m-values are somewhat involved and will be presented elsewhere.

6.1. Computational procedure

A Rayleigh-Ritz variational method will be employed throughout. The formalism is as follows. Let ξ_i denote an eigensolution of Eq. (3), with the corresponding eigenvalue $\omega_i^2=\varepsilon_i$. The subscript i tentatively denotes the set of all specifications of the eigensolution (the s-, p-, t-types, the harmonic numbers l, m, and the radial wave number, k). The ξ_i is a vector in the Hilbert space H of Sects. 3–5. Let $\{\zeta_j\}$ by a basis for H, where j also stand for similar specifications of the element in question. Expand ξ_i in terms of $\{\zeta_j\}$:

$$\xi_i=\sum_j \zeta_j Z_{ji}, \tag{21}$$

where Z_{ji} are constants of expansion and will be treated as variational parameters. Substituting Eq. (21) in Eq. (3) or in its equivalent differential form, Eq. (1b), gives the following matrix equation

$$WZ=SZE. \tag{22}$$

or

$$Z^\dagger SZ=I, \tag{22a}$$

and

$$Z^\dagger WZ=E, \tag{22b}$$

where I is a unit matrix, E is a diagonal matrix whose elements are the eigenvalues ε_i, Z is the matrix of the variational constants Z_{ji}. The elements of S are (see Eq. [6a]).

$$S_{ij}=\int \Phi 2\zeta_i^*\cdot\zeta_j\, dV. \tag{23a}$$

For the W-matrix one has

$$W=W_1+\operatorname{sign}(dF/dE)\,W_2, \tag{23b}$$

where the elements of $W1$ and $W2$ are (see Eq. [6b] and [6c]).

$$W1_{ij}=\int \Phi 4\,[\partial_\nu\zeta_i^{\mu *}\partial^\nu\zeta_j^\mu+2\partial_\nu\zeta_i^{\mu *}\partial_\mu\zeta_j^\nu]\,dx + \int \Phi 2\partial^2_{\mu\nu}U\zeta_i^{\mu *}\zeta_j^\nu\,dx, \tag{23c}$$

$$W2_{ij}=G\int V\cdot(\Psi\zeta_i^*)\,V'\cdot(\Psi\zeta_j)'\,|x-x'|\,dx\,dx'. \tag{23d}$$

The matrices S, $W1$, $W2$ are known. A solution of Eq. (22) consists of finding the eigenvalue matrix E and the eigenvector matrix Z for the given S and W matrices.

In integrating Eqs. (23), some of the integrals over (θ, ϕ) angles vanish. The properties (i)–(iv) listed in the beginning of this section are inferred from these vanishing matrix elements.

A Rayleigh-Ritz approximation consists of truncating the series expansion of Eq. (21) at some finite number of terms n, say. This, correspondingly, scoops out a finite dimensional vector space $H(n)$ out of the infinite dimensional H. All matrices in $H(n)$ are $n\times n$. Solution of Eq. (22) reduces to simultaneous diagonalization of S to I and of W to E, and to finding the matrix Z of the transformation. This procedure will be carried out here. However, due to the multitude of the subspaces of H, each with its own idiosyncracies, the bookkeeping of the modes is elaborate and requires special precautions.

6.2. Partitioning of Eqs. (22)

In long-hand notation an element of the basis set reads $\zeta_{\alpha lmk}$ (see Eqs. [13] and [20] and Sect. 1, Notation), where α denotes one of the s-, p-, or t-types, l and m are spherical harmonic numbers, and k is the radial number of Eqs. (20). By property (ii) above an eigensolution of Eq. (22) always has a definite m-symmetry which remains unchanged throughout the analysis. By property (iv), if $|m|=0$ or ± 1, the eigenmodes also have a definite l-symmetry. To simplify the notation. Both of these indices will be suppressed, hereafter. The column vector of the basis sets for H can now be written as follows:

$$(\zeta_{si}|\zeta_{pj}|\zeta_{tk}),\qquad i,j,k=1,2,\ldots, \tag{24a}$$

where we have explicitly *partitioned* the set into its scaloidal, poloidal, and toroidal components, and i, j, k are radial wave number designations. Any of the matrices of Eq. (22) gets *block-partitioned*, correspondingly. Thus,

$$M=\begin{bmatrix} M_{ss} & M_{sp} & M_{st} \\ M_{ps} & M_{pp} & M_{pt} \\ M_{ts} & M_{tp} & M_{tt} \end{bmatrix},\qquad M=E, Z, W1, W2, S. \tag{24b}$$

There are simplifications, however. Perturbations of different s-, p-, t-types are orthogonal in H in the sense of Eq. (11). Therefore the S-matrix is block diagonal:

$$S=\begin{bmatrix} S_{ss} & & \\ & S_{pp} & \\ & & S_{tt} \end{bmatrix}. \tag{25a}$$

In Eq. (25a) and in what follows the blank slots are zero. From the property (iv), there is no coupling between t-types and s- or p-types. Therefore, the W-matrix takes the following form:

$$W=\begin{bmatrix} W_{ss} & W_{sp} & \\ W_{ps} & W_{pp} & \\ & & W_{tt} \end{bmatrix}. \tag{25b}$$

The matrix of the eigenvalues, E, is by definition block-diagonal:

$$E=\begin{bmatrix} E_s & & \\ & E_p & \\ & & E_t \end{bmatrix}. \tag{26a}$$

Substituting Eqs. (25) and (26a) in Eq. (22) gives the corresponding block-structure of Z, which turns out to be the same as that of W:

$$Z=\begin{bmatrix} Z_{ss} & Z_{sp} & \\ Z_{ps} & Z_{pp} & \\ & & Z_{tt} \end{bmatrix}. \tag{26b}$$

Equation (22) itself splits as follows:

$$\begin{bmatrix} W_{ss} & W_{sp} \\ W_{ps} & W_{pp} \end{bmatrix}\begin{bmatrix} Z_{ss} & Z_{sp} \\ Z_{ps} & Z_{pp} \end{bmatrix}=\begin{bmatrix} S_{ss} & \\ & S_{pp} \end{bmatrix}\begin{bmatrix} Z_{ss} & Z_{sp} \\ Z_{ps} & Z_{pp} \end{bmatrix}\begin{bmatrix} E_s & \\ & E_p \end{bmatrix} \tag{27a}$$

and

$$W_{tt}Z_{tt}=S_{tt}Z_{tt}E_{tt}. \tag{27b}$$

6.3. Explicit expressions for the S- and W-matrices

6.3.1. The scaloidal and/or poloidal elements

The angular dependence of ζ_s and ζ_p is the same. This allows one to present the matrix elements constructed with these vectors by a single expression. Let the r-dependent part of the radial component of $\zeta_{\alpha k}, \alpha = s, p$, be denoted by $\zeta_{\alpha kr}$, and that of its non-radial component by $\zeta_{\alpha k\perp}$. From Eqs. (13a) and (13b) one reads:

$$\zeta_{skr} = -\chi'_{sk}, \tag{28a}$$

$$\zeta_{sk\perp} = -\frac{1}{r}\chi_{sk}, \tag{28b}$$

$$\zeta_{pkr} = \frac{1}{\Phi 2}\frac{l(l+1)}{r^2}\chi_{pk}, \tag{29a}$$

$$\zeta_{pk\perp} = \frac{1}{\Phi 2}\frac{1}{r}\chi'_{pk}, \tag{29b}$$

where a "prime" denotes d/dr. The (i,j) element of a matrix block $S_{\alpha\beta}$ or $W_{\alpha\beta}$ is obtained by inserting the pair of vectors $\zeta^*_{\alpha i}$ and $\zeta_{\alpha j}$ in Eqs. (23) and integrating over the (θ,ϕ) angles. The angular integrals are elementary but elaborate. With the notation of Eqs. (28) and (29) one obtains

$$S_{\alpha i\alpha j}=\int \Phi 2\,[\zeta_{\alpha ir}\zeta_{\alpha jr}+l(l+1)\zeta_{\alpha i\_}\zeta_{\alpha j\_}]\,r^2\,dr, \qquad \alpha = s, p. \tag{30}$$

All integrals in Eqs. (30)–(35) are from 0 to R. The expression for $W1$ is:

$$\begin{aligned} W1_{\alpha i\beta j} &= W1_{\beta j\alpha i} \\ &= 3\int \Phi 4\,[r^2\zeta'_{\alpha ir}\zeta'_{\beta jr}+\zeta_{\alpha ir}\zeta_{\beta jr}]\,dr \\ &\quad + l(l+1)\int \Phi 4\,[(\zeta_{\alpha ir}-\zeta_{\alpha i\perp})(\zeta_{\beta jr}-\zeta_{\beta j\perp})+r^2\zeta'_{\alpha i\perp}\zeta'_{\beta j\perp} \\ &\quad + 2r(\zeta_{\alpha ir}-\zeta_{\alpha i\perp})\zeta'_{\beta j\perp}+2r\zeta'_{\alpha i\perp}(\zeta_{\beta jr}-\zeta_{\beta j\perp}) \\ &\quad - 3(\zeta_{\alpha ir}\zeta_{\beta j\perp}+\zeta_{\alpha i\perp}\zeta_{\beta jr})+3(l^2+l-1)\,\zeta_{\alpha i\perp}\zeta_{\beta j\perp}]\,dr \\ &\quad + \int \Phi 2\,[r^2U''\zeta_{\alpha ir}\zeta_{\beta jr}+l(l+1)\,rU'\zeta_{\alpha i\perp}\zeta_{\beta j\perp}]\,dr, \\ &\quad \alpha,\beta = s, p. \end{aligned} \tag{31}$$

The $W2$-matrix expresses the effect of the perturbation in self-gravitation. It is exactly the same as the corresponding term for a fluid. From Eq. (9.10d) and (9.7a) of Sobouti (1980) one finds

$$W2_{\alpha i\beta j}=W2_{\beta j\alpha i}=4\pi G\int \mathscr{Y}_{\alpha i}\mathscr{Y}_{\beta j}\,dr, \qquad \alpha,\beta = s, p. \tag{32}$$

where

$$\mathscr{Y}_{\alpha i}(r)=r\Psi\zeta_{\alpha ir}-(l+1)\,r^l\int_r^R \Psi\,[\zeta_{\alpha ir}-l\zeta_{\alpha\perp}]\,r^{-1}\,dr, \quad \alpha = s, p. \tag{32a}$$

6.3.2. The toroidal elements

The toroidal vectors of Eq. (13c) have non-radial components only. Let the radius-dependent part of this be denoted as

$$\zeta_{ti\perp}=\frac{1}{\Phi 2}\frac{1}{r}\chi_{tli}(r). \tag{33}$$

With this notation, inserting a pair of vectors ζ^*_{ti} and ζ_{tj} of Eq. (13c) in Eqs. (23) and integrating over the angles gives

$$S_{ti\,tj} = l(l+1)\int \Phi 2\,\zeta_{ti\perp}\zeta_{tj\perp}r^2\,dr, \tag{34}$$

$$\begin{aligned} W1_{ti\,tj} &= l(l+1)\int \Phi 4 \\ &\quad \cdot[(r\zeta'_{ti\perp}-\zeta_{ti\perp})(r\zeta'_{tj\perp}-\zeta_{tj\perp})+(l^2+l-2)\zeta_{ti\perp}\zeta_{tj\perp}]\,dr, \end{aligned} \tag{35}$$

$$W2_{ti\,tj}=0. \tag{36}$$

Once again let it be restated that there is no coupling between the toroidal fields and the other types in the case of $m=0$ and 1. Therefore, the mixed ts- and tp-blocks of all the matrices vanish identically.

7. Volume and surface density waves

By Eq. (14) a vector ξ is proportional to the Lagrangian displacement of a material element of the system. Corresponding to this displacement is the Eulerian density change of Eq. (15a). For a scaloidal-poloidal vector ξ belonging to harmonic numbers (l, m), Eq. (13a) gives

$$\delta\varrho(r,\theta,\phi)=\delta\varrho(r)\;Y_{lm}(\theta,\phi), \tag{37}$$

where

$$\delta\varrho(r)=\frac{i}{\omega}\left[\frac{1}{r^2}\frac{d}{dr}(r^2\xi_r)-l(l+1)\frac{1}{r^2}\xi_\perp\right]. \tag{37a}$$

For a toroidal displacement the density change vanishes identically. The density change of Eqs. (37) generated by an eigenmode ξ will be referred to as a *volume density wave*.

More important than $\delta\varrho$, and perhaps of relevance to surface brightness inhomogeneities of globular clusters, is the projection of $\delta\varrho$ on some plane (the plane of sky, say). Let P be a plane normal to which makes an angle α with the z-axis and the intersection of which with the xy-plane makes an angle β with the x-axis. Let (x', y', z') be a new coordinate system where z' is the normal to P and x' is the intersection of P with xy. The angles β and α are the first two Euler angles which transforms (x, y, z) to (x', y', z'). The law of transformation from the spherical polar coordinates (r, θ, ϕ) on (x, y, z) to (r', θ', ϕ') on (x', y', z') is

$$r=r', \tag{38a}$$

$$\cos\theta = \cos\theta'\cos\alpha+\sin\theta'\sin\alpha\cos(\phi'+\beta), \tag{38b}$$

$$\tan\phi=\frac{\cos\theta'\sin\alpha+\sin\theta'\cos\alpha\sin(\phi'+\beta)}{\sin\theta'\cos(\phi'+\beta)} \tag{38c}$$

The volume density wave of Eq. (37) projected on P and integrated over the available z' values gives

$$\delta\sigma(\bar{\omega}',\phi') = \int_{-z_0}^{z_0} \delta\varrho(r)\, Y_{lm}(\theta,\phi)\, dz' \tag{39}$$

where $\bar{\omega}'$ and ϕ' are two-dimensional circular polar coordinates on P. The integration limits are $\pm z_0 = \pm\sqrt{R^2-\bar{\omega}^2}$. The projected density change of Eq. (39) will be referred to as a *surface density wave*.

For $l=0$, $m=0$ all planes of projection are equivalent. Equation (39) takes the simple form

$$\delta\sigma(\bar{\omega}) = 2\int_0^{z_0} \delta\varrho(r)\, dz, \qquad l=0. \tag{40}$$

For $l=1$, $m=0$, one has $Y_{10}\propto\cos\theta$. Substituting for $\cos\theta$ from Eq. (38b) and noting the symmetry of the integrand with respect to $\pm z'$ gives

$$\delta\sigma(\bar{\omega}',\phi') = \sin\alpha\cos(\phi'+\beta)\int_{-z_0}^{z_0} \delta\varrho(r)\sin\theta'\, dz', \tag{41}$$

where $r^2=\bar{\omega}'^2+z'^2$ and $\sin\theta'=\bar{\omega}'/\sqrt{\bar{\omega}'^2+z'^2}$. The integral in Eq. (41) is independent of α and β. Therefore the pattern of the surface density waves of $l=1$ is independent of the orientation of the plane on which it is projected. The amplitude of the waves, however, is proportional to $\sin\alpha\cos(\phi'+\beta)$.

The case $l=1$, $m=1$ is the same as $l=1$, $m=0$. For, real Y_{10} ($\propto\cos\theta$) transforms to *real* Y_{11} ($\propto\cos\theta\cos\phi$) upon interchanging the x and y axes. This is equivalent to letting $\alpha=\pi/2$ and $\beta=0$ in Eqs. (38). The same is true for $l=1$, $m=-1$, which could result from Y_{10} by interchanging the y and z axes. Therefore, we conclude that in the case of $l=1$, $m=0,\pm1$, the surface density wave pattern on the plane of sky is independent from orientation of any preferred polar axis. Only the amplitude of the surface waves depends on this orientation.

This simplifying feature does not hold for higher l-values. For this reason we have further confined the numerical results of the paper to $l=0$, and $l=1$, $m=0,\pm1$. The results for higher l-values will be given elsewhere.

8. Numerical results

The eigenmodes of polytropic stellar systems for $l=0$, and 1 are calculated. Polytropes have a constant polytropic index, n, throughout the system. Numerical experiments showed that the alternative ansatz of Eqs. (42) below were more suitable than those of Eqs. (20). Convergence of the eigenvalues and the eigenvectors was faster. And the eigenvalues converged to lower values. Thus:

$$\chi_{slk} = |r^2-R^2|^{(2n-1)/4} r^{l+2k}, \qquad k=0,1,2,\ldots, \tag{42a}$$

$$\chi_{plk} = |r^2-R^2|^{(2n+9)/4} r^{l+2k+1}, \qquad k=0,1,2,\ldots, \tag{42b}$$

$$\chi_{tlk} = |r^2-R^2|^{(2n+5)/4} r^{l+2k+1}, \qquad k=0,1,2,\ldots, \tag{42c}$$

The surface- and the center-behaviors of Eqs. (42) and of Eqs. (20) are identical. The functions $\Phi 2$, $\Phi 4$, and Ψ for polytropes were taken from Sect. 4 of Paper I. Sample computations are presented in tabulated and graphic forms below.

8.1. *The radial modes, $l=0$*

These are purely scaloidal fields. For by Eqs. (13b) and (13c) there are no poloidal or toroidal vectors corresponding to $l=0$. The first five eigenvalues of polytropes 1.0 to 4.5, in five variational orders are given in Table 1. The eigenvalues here and in other tables are in units of $4\pi G\varrho_c$. A number $a\,10^{\pm b}$ here and in other tables is written as $a\pm b$. As a rule convergence of the variational results is better for lower central concentrations, i.e., for lower polytropic indices. As a sample, the eigenvectors (i.e., the variational constants of Eq. [21], Z_{ji}) of polytropes 1.0, 1.5, 2.0, and 2.5 are given in Table 2.

Table 1. Eigenvalues of radial oscillations of polytropes

.3834+1				n=1.0, l=0
.2929+1	.5600+1			
.2655+1	.4636+1	.8404+1		
.2558+1	.4296+1	.6957+1	.1131+2	
.2523+1	.4189+1	.6468+1	.9593+1	.1522+2
.8987				n=1.5, l=0
.6441	.2072+1			
.5879	.1649+1	.4052+1		
.5624	.1527+1	.3145+1	.6100+1	
.5491	.1485+1	.2884+1	.4875+1	.8975+1
.4152				n=2.0, l=0
.2630	.1232+1			
.2279	.9063	.2584+1		
.2112	.8101	.1829+1	.3984+1	
.2021	.7742	.1612+1	.2918+1	.6001+1
.2779				n=2.5, l=0
.1624	.7923			
.1367	.5197	.1655+1		
.1253	.4440	.1045+1	.2564+1	
.1191	.4156	.8772	.1683+1	.3878+1
.1956				n=3.0, l=0
.1054	.4790			
.8679-1	.2732	.9715		
.7917-1	.2228	.5358	.1503+1	
.7500-1	.2044	.4277	.8639	.2268+1
.1219				n=3.5, l=0
.5624-1	.2524			
.4415-1	.1215	.4867		
.3946-1	.9467-1	.2290	.7460	
.3694-1	.8510-1	.1740	.3646	.1115+1
.5797-1				n=4.0, l=0
.1953-1	.1041			
.1417-1	.3869-1	.1868		
.1224-1	.2839-1	.7042-1	.2773	
.1125-1	.2481-1	.5058-1	.1091	.4051
.1419-1				n=4.5, l=0
.2516-2	.2331-1			
.1698-2	.4935-2	.3907-1		
.1418-2	.3369-2	.9035-2	.5495-1	
.1283-2	.2847-2	.6009-2	.1384-1	.7673-1

The present computations use the surface boundary conditions of Eqs. (18). Similar computations given in Tables 1 and 3 of Paper I use different surface conditions. A comparison of the present results with those of Paper I shows a few per cent increase in the eigenvalues of polytropes 1.0 and 1.5. As the polytropic index increases, however, the difference grows and amounts to a factor of two in polytropes 4.0 and 4.5.

The corresponding volume and surface density waves are calculated from Eqs. (37) and (40). Sample plots of these quantities as functions of the spherical radius, r, and the cylindrical radius, $\bar{\omega}$, are given in Figs. 1–3. The plots are for polytropes 1.0, 1.5, and 2.0. The modes are arranged in an ascending sequence of eigenvalues and are numbered from $k=1-5$. The k-index could properly be interpreted as a radial wave number. An increase in k by one unit adds one more node to the waves. On the whole, as the central condensation increases, the outward extension of the waves diminishes.

Table 2. Eigenvalues and eigenvectors of radial oscillations of polytropes

```
 n=1, l=0 :
  .2523+1  .4189+1  .6468+1  .9593+1  .1522+2

  .1388+1-.1944+1  .1018+2-.9715+1-.5025+2
-.5744+1-.1699+2-.3087+2-.4086+2  .3529+3
  .3558+2  .5601+2  .1318+3  .3377+3-.1008+4
-.5766+2-.1093+3-.2884+3-.6197+3  .1241+4
  .4371+2  .8410+2  .1952+3  .3423+3-.5496+3

 n=1.5, l=0 :
  .5491    .1485+1  .2884+1  .4875+1  .8975+1

  .4561+1-.5536+1  .1310+2  .1229+2-.5849+2
-.2962+1-.1500+2-.3963+2  .3891+2  .4568+3
  .4047+2  .6699+2  .1461+3-.4442+3-.1437+4
-.6975+2-.1219+3-.3659+3  .9311+3  .1921+4
  .5441+2  .1056+3  .2900+3-.5671+3-.9159+3

 n=2.0, l=0 :
  .2021    .7742    .1612+1  .2918+1  .6001+1

  .7233+1-.6582+1  .1486+2  .1274+2-.6978+2
-.2600+1-.2149+2-.5100+2  .7351+2  .5925+3
  .5862+2  .1089+3  .2313+3-.7199+3-.2011+4
-.1096+3-.2197+3-.6415+3  .1551+4  .2868+4
  .9567+2  .2088+3  .5401+3-.9836+3-.1453+4

 n=2.5, l=0 :
  .1191    .4156    .8772    .1683+1  .3878+1

  .9250+1-.7344+1  .1668+2  .1307+2  .8488+2
-.1372+1-.3430+2-.6242+2  .1357+3-.7831+3
  .9289+2  .1732+3  .3763+3-.1199+4  .2855+4
-.1837+3-.3997+3-.1160+4  .2634+4-.4330+4
  .1826+3  .4225+3  .1023+4-.1726+4  .2321+4

 n=3.0, l=0 :
  .7500-1  .2044    .4277    .8639    .2268+1

  .1046+2-.8583+1-.1923+2-.1416+2  .1067+3
  .9692   -.5681+2  .7284+2-.2391+3-.1075+4
  .1626+3  .2716+3-.6202+3  .2032+4  .4208+4
-.3384+3-.7339+3  .2122+4-.4578+4-.6780+4
  .3869+3  .8568+3-.1954+4  .3104+4  .3839+4
```

In Figs. 4 and 5 the surface waves of Eq. (40) are plotted as a cloud of dots on a disk. The density of dots is proportional to $[\delta\sigma(\bar{\omega}) - \delta\sigma_{\min}]/(\delta\sigma_{\max} - \delta\sigma_{\min})$, where the subscripts min and max indicate the minimum and maximum values of $\delta\sigma$. The maximum dot density corresponds to maximum Eulerian mass density changes, and the zero dot density corresponds to the minimum mass density changes. Due to a coarse digitization process (from 0 to 8 or 10) the finer details of $\delta\sigma$ as a function of $\bar{\omega}$ are smeared out. Should a globular cluster have a density wave of the type contemplated here, then Figs. 4 and 5, and similar ones to come later, could mimic the surface brightness fluctuations of it.

8.2. *The non-radial modes of* $l=1$

As pointed out earlier, these modes are either of purely toroidal nature or of mixed scaloidal-poloidal character. Each is introduced separately.

8.2.1. Scaloidal-poloidal modes of $l=1$

At most, ten variational parameters are used in the computations, five for scaloidal and five for poloidal trial functions. The eigenvalues in ten different variational orders are given in Table 3.

The tenth order eigenvectors of polytropes 1.0, 1.5, and 2.0 are given in Tables 4, 5, and 6, respectively. The eigenvalues are displayed in the line marked by the first asterisk. The column of ten entries below an eigenvalue is its corresponding eigenvector. An entry in the line marked by p1 (or s1) is the variational coefficient corresponding to the first poloidal (or scaloidal) ansatz of Eq. (20b) or (20a). Entries in other lines have similar interpretations.

To appraise the degree of coupling between the scaloidal and poloidal motions, computations using pure poloidal or pure scaloidal ansatz are also presented in Tables 4–6. The eigenvalues displayed in the line marked by the second asterisk are calculated with pure poloidal ansatz. The corresponding eigenvectors, columns of five entries, are below each eigenvalue. The eigenvalues in the line marked by the third asterisk and the columns following them are calculated with five scaloidal trial functions. The columns of pure-ansatz calculations are displaced to match those of the mixed-ansatz calculations as closely as possible. Interesting conclusions may be drawn. For example, let us compare the tenth mode (i.e., the tenth column) of Table 4 with its pure scaloidal counterpart. The two eigenvalues differ in the fourth figures (12.93 as compared with 12.92). The scaloidal component of the mixed calculation (that is, the last five entries marked by s1 to s5) is surprisingly the same as the eigenvector of the pure calculations. The poloidal component of the mixed calculation (that is, the first five entries marked by p1 to p5) do not have counterparts in pure calculations. They are, however, much smaller than the scaloidal components. Thus, in the loose sense of the word, this mode is classified as a *scaloidal* mode, and is marked by an s at the bottom of the column. The same can be said of the 9th, 8th, and 6th modes, except that the differences between the mixed and pure calculations have become slightly larger. These are also marked as scaloidal modes. The same can also be said of the 7th, 5th, and 4th modes, except that the scaloidal components and the poloidal components have exchanged their roles. These are marked as *poloidal* modes. On the other hand, in the first two columns one encounters a strong mixing of the poloidal and scaloidal ansatz. The first mode, in particular, has comparable poloidal and scaloidal components. It is marked as an sp mode.

The radial dependence of the volume density waves, Eq. (37a), and the radial dependence of the surface density waves, the integral in Eq. (41), are plotted in Figs. 6–8. The modes are arranged in an ascending sequence of the eigenvalues and are numbered from $k=1$ to 10. Unlike the $l=0$ case, k may not be considered as a proper radial wave number. The number of nodes does not necessarily increase with k. This is due to the bispectral nature of the modes belonging to each $l \geqq 1$. Of the two modes with the same number of nodes, one usually is dominantly of scaloidal type and the other is dominantly of poloidal type. For the example, in Fig. 6, the number of nodes (not counting the center) for $k=1$ and $k=6$ is two, and they are of sp and s types, respectively. That for $k=2$ and $k=3$ is three and they are of p and s types, respectively.

In Figs. 9 and 10, the surface density of Eq. (41) is digitized and plotted as clouds of dots. The darkest and the lightest areas of the plots correspond to the maxima and minima of the Eulerian density fluctuations projected on a plane. The asymmetry of the plots is simply the effect of $\cos\phi'$ in Eq. (41).

8.2.2. Toroidal modes

The eigenvalues of five toroidal modes of $l=1$ in five variational orders are reported in Table 7. They are in units of $4\pi G\varrho_c$. The lowest eigenvalue is zero for polytrope 2.5, and appears to converge to zero in other polatropes. This is because of the special form of the first toroidal ansatz. Equations (20c) and

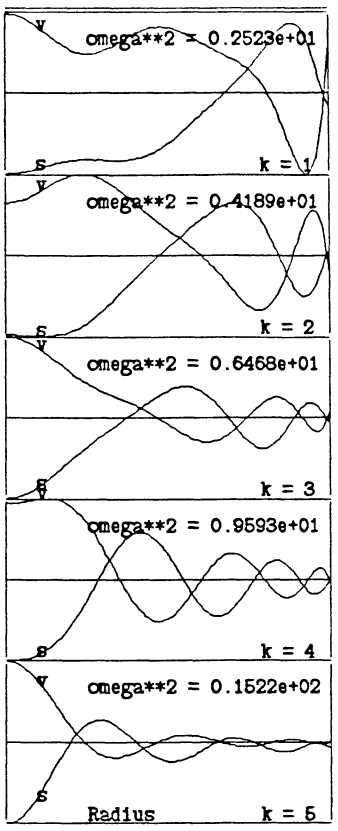

Fig. 1. Radial dependence of volume (v) and of surface (s) density waves; $n=1.0$, $l=0$

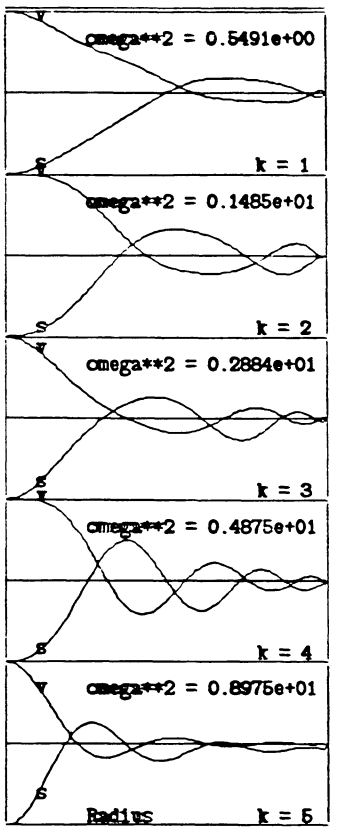

Fig. 2. Radial dependence of volume (v) and of surface (s) density waves; $n=1.5$, $l=0$

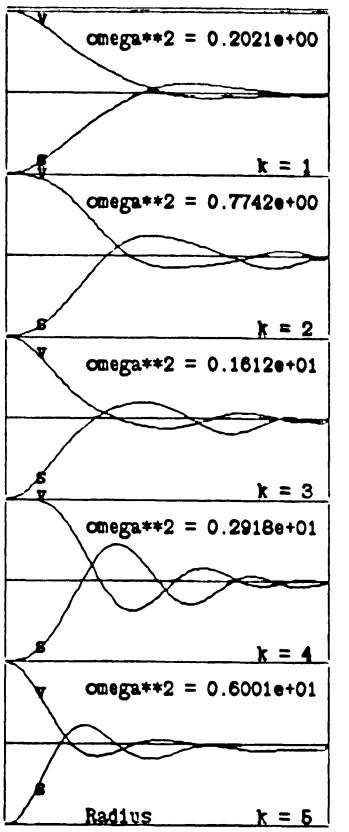

Fig. 3. Radial dependence of volume (v) and of surface (s) density waves; $n=2.0$, $l=0$

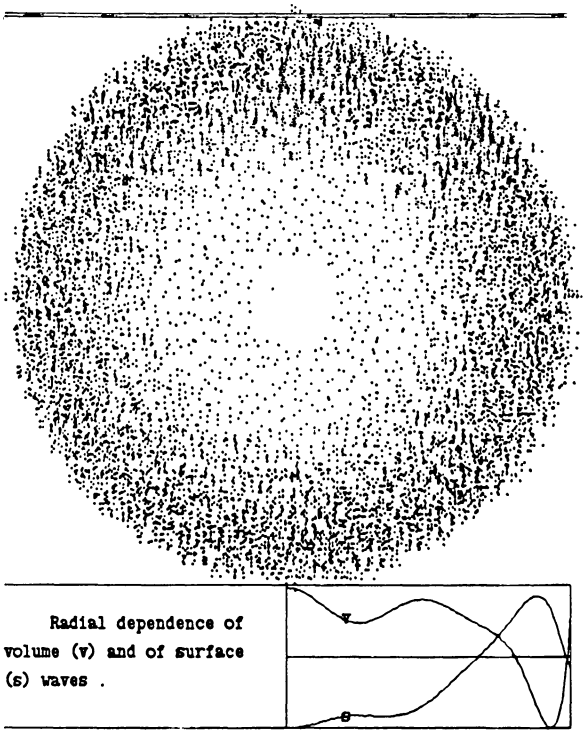

Fig. 4. A surface density wave of the polytrope $n=1.0$; the radial mode $l=0$, $k=1$, $\omega^2=0.2523\,\mathrm{E}+01$. The density of dots is zero at minimum mass density and is maximum at maximum mass density

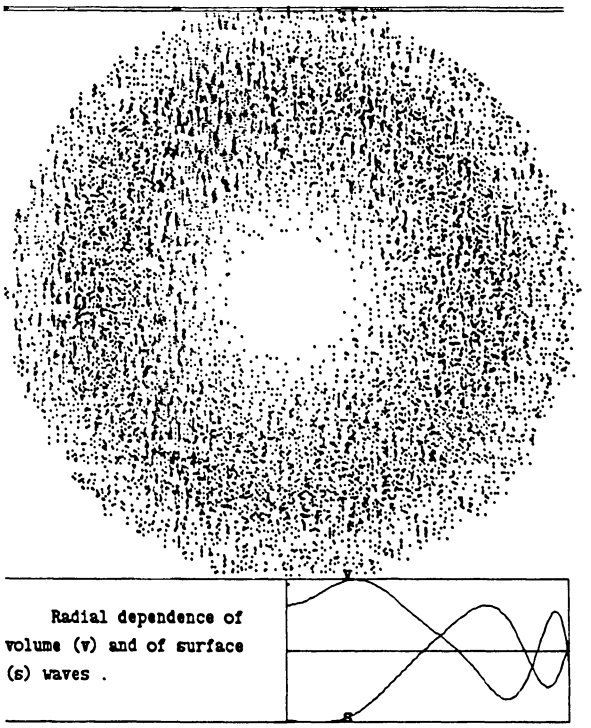

Fig. 5. A surface density wave of the polytrope $n=1.0$; the radial mode $l=0$, $k=2$, $\omega^2=0.4189\,\mathrm{E}+01$. The density of dots is zero at minimum mass density and is maximum at maximum mass density

Table 3. Eigenvalues of non-radial oscillations of polytropes. Scaloidal-poloidal modes

.5879	.1716+1								n=1.0, l=1
.2273	.1252+1	.1375+1	.4285+1						
.2072	.8396	.1140+1	.2298+1	.3439+1	.6637+1				
.2040	.8339	.1104+1	.1589+1	.3170+1	.3411+1	.5472+1	.9499+1		
.2029	.8308	.1089+1	.1581+1	.2526+1	.3085+1	.4708+1	.5085+1	.7970+1	.1293+2
.2545	.3190								n=1.5, l=1
.1445	.2169	.6125	.1423+1						
.1241	.1950	.4928	.1047+1	.1120+1	.2932+1				
.1190	.1872	.4905	.9408	.1036+1	.1577+1	.2311+1	.4907+1		
.1179	.1829	.4873	.9376	.1005+1	.1508+1	.2129+1	.2214+1	.3890+1	.7342+1
.7596-1	.1387								n=2.0, l=1
.3547-1	.1015	.2982	.8450						
.2818-1	.8180-1	.2682	.5190	.6321	.1851+1				
.2471-1	.7472-1	.2647	.5089	.5646	.8159	.1347+1	.3195+1		
.2301-1	.7249-1	.2619	.5062	.5402	.8158	.1180+1	.1208+1	.2326+1	.4871+1
.4552-1	.6457-1								n=2.5, l=1
.1450-1	.5625-1	.1473	.5697						
.8467-2	.4736-1	.1399	.2589	.3764	.1210+1				
.5914-2	.4304-1	.1344	.2587	.3206	.4172	.7855	.2076+1		
.4543-2	.4115-1	.1324	.2536	.2986	.4134	.6214	.6676	.1355+1	.3157+1
.2756-1	.3953-1								n=3.0, l=1
.1311-1	.2692-1	.6765-1	.3631						
.8408-2	.2383-1	.6630-1	.1205	.2008	.7351				
.6438-2	.2251-1	.6162-1	.1201	.1620	.1946	.4103	.1241+1		
.5284-2	.2143-1	.6078-1	.1133	.1473	.1905	.2923	.3294	.7067	.1869+1
.1036-1	.3102-1								n=3.5, l=1
.1014-1	.1155-1	.2607-1	.1964						
.7896-2	.1002-1	.2582-1	.4740-1	.8677-1	.3810				
.6519-2	.9846-2	.2349-1	.4656-1	.6640-1	.7632-1	.1743	.6335		
.5453-2	.9681-2	.2337-1	.4218-1	.5911-1	.7347-1	.1142	.1321	.3010	.9424
.2891-2	.2014-1								n=4.0, l=1
.2765-2	.6997-2	.7392-2	.7896-1						
.2448-2	.5340-2	.6869-2	.1302-1	.2606-1	.1462				
.2424-2	.5520-2	.6295-2	.1248-1	.1909-1	.2123-1	.5092-1	.2393		
.2295-2	.5279-2	.6244-2	.1102-1	.1670-1	.1979-1	.3133-1	.3701-1	.8781-1	.3515
.3406-3	.9850-2								n=4.5, l=1
.2949-3	.7647-3	.2381-2	.1921-1						
.2570-3	.7334-3	.1430-2	.1789-2	.4177-2	.3057-1				
.2570-3	.6493-3	.1307-2	.1440-2	.2386-2	.3161-2	.6900-2	.4629-1		
.2479-3	.6471-3	.1154-2	.1318-2	.2148-2	.2586-2	.3626-2	.5039-2	.1101-1	.6526-1

Table 4. Normal modes of $l=1$ calculated with mixed and pure scaloidal-poloidal ansatz. Polytrope 1.0

*	.2029	.8308	.1089+1	.1581+1	.2526+1	.3085+1	.4708+1	.5085+1	.7970+1	.1293+2
p1	.1270+1	.1722+1	.5190-2	-.1982+1	-.3003+1	.5436-1	.1551+1	-.4851-2	-.3690-1	.7303-1
p2	-.2230+1	-.6892+1	-.1091+1	.1242+2	.3199+2	.4564	-.2051+2	-.2141	.1717	-.8047
p3	.1334+1	.7675+1	.1577+1	-.1860+2	-.1041+3	-.2569+1	.8244+2	.1457+1	.9765-1	.2744+1
p4	-.2345	-.4415+1	-.6150	.2071+1	.1306+3	.3819+1	-.1279+3	-.2966+1	-.8354	-.3668+1
p5	-.1279	.1861+1	.1216	.5947+1	-.5521+2	-.1770+1	.6713+2	.1824+1	.6281	.1680+1
s1	.7746	-.4068	.1853+1	.8419-1	.1388	-.1751+1	-.1707	.2905+1	-.3006+1	.7584+1
s2	.8951-1	.2416	.3018	-.5062-1	-.1445+1	-.3509+1	.1356+1	-.9803+1	.8274-1	-.9487+2
s3	.2345+1	-.2909+1	.8876+1	-.1529+1	.5103+1	.1906+2	-.6088+1	.3512+2	.1002+3	.3636+3
s4	-.4128+1	.5669+1	-.1580+2	.5303+1	-.6363+1	-.3946+2	.1193+2	-.1056+3	-.2587+3	-.5404+3
s5	.3634+1	-.5321+1	.1421+2	-.3800+1	.2153+1	.3947+2	-.7629+1	.9061+2	.1730+3	.2727+3
	sp	p	s	p	p	s	p	s	s	s

Pure poloidal ansatz :

*	.2973	.8468	.1584+1	.2530+1	.4710+1		
p1	.1377+1	.1647+1	-.1977+1	-.3003+1	.1551+1		
p2	-.2498+1	-.6894+1	.1240+2	.3200+2	-.2052+2		
p3	.1588+1	.7805+1	-.1851+2	-.1041+3	.8253+2		
p4	-.4214	-.4491+1	.1943+1	.1306+3	-.1280+3		
p5	-.3688-1	.1885+1	.6002+1	-.5519+2	.6721+2		

Pure scaloidal ansatz :

*	.9895	.3076+1	.5082+1	.7967+1	.1292+2	
s1	.2059+1	-.1748+1	.2904+1	-.3008+1	.7585+1	
s2	.2679	-.3466+1	-.9823+1	.6869-1	-.9489+2	
s3	.9419+1	.1895+2	.3528+2	.1002+3	.3637+3	
s4	-.1678+2	-.3931+2	-.1060+3	-.2588+3	-.5405+3	
s5	.1514+2	.3945+2	.9088+2	.1730+3	.2728+3	

Table 5. Normal modes of $l=1$ calculated with mixed and pure scaloidal-poloidal ansatz. Polytrope 1.5

Mixed scaloidal - poloidal ansatz :

*	.1179	.1829	.4873	.9376	.1005+1	.1508+1	.2129+1	.2214+1	.3890+1	.7342+1
p1	.1365+1	-.1712	-.1492+1	.1705+1	-.2213	-.2467+1	.9460-1	-.2302+1	-.2866	.1297
p2	-.3388+1	.2610	.6820+1	-.1021+2	.3808	.2415+2	.8154	.2877+2	.2446+1	-.1426+1
p3	.4026+1	-.1277	-.9999+1	.1405+2	.2665-1	-.7140+2	-.6294+1	-.1110+3	-.6763+1	.4943+1
p4	-.2606+1	-.6073-1	.8619+1	-.2739	-.8032-1	.7939+2	.1141+2	.1671+3	.7543+1	-.6772+1
p5	.6421	.8062-1	-.3764+1	-.4697+1	-.1162	-.2829+2	-.6245+1	-.8568+2	-.2951+1	.3190+1
s1	.9543-1	.3090+1	.5855	-.3230	-.2304+1	.3357	.3246+1	.6826-1	-.3230+1	.8212+1
s2	.4908	.1203+1	-.1436+1	.1330+1	-.8643	-.2914+1	-.1449+2	-.2555+1	.5028+1	-.1181+3
s3	.4557+1	.8653+1	.1571+1	.2242+1	.2383+2	.5300+1	.3786+2	.1009+2	.1185+3	.5067+3
s4	-.8121+1	-.1649+2	-.5195+1	-.8910+1	-.4329+2	.6898	-.1219+3	-.8582+1	-.3729+3	-.8269+3
s5	.8176+1	.1609+2	.5574+1	.4687+1	.4862+2	-.3956+1	.1275+3	-.1360+1	.2826+3	.4528+3
	sp	s	p	p	s	p	s	p	s	s

Pure poloidal ansatz :

*	.1375	.5010	.9489	.1517+1	.2219+1
p1	.1348+1	-.1510+1	.1712+1	-.2482+1	-.2319+1
p2	-.3210+1	.6726+1	-.1006+2	.2415+2	.2902+2
p3	.3677+1	-.9718+1	.1330+2	-.7094+2	-.1120+3
p4	-.2285+1	.8459+1	.7375	.7833+2	.1683+3
p5	.5165	-.3765+1	-.5103+1	-.2765+2	-.8620+2

Pure scaloidal ansatz :

*	.1815	.9857	.2113+1	.3874+1	.7334+1
s1	.3074+1	-.2381+1	.3268+1	-.3253+1	.8213+1
s2	.1219+1	-.7096	-.1444+2	.5356+1	-.1182+3
s3	.9397+1	.2373+2	.3673+2	.1174+3	.5071+3
s4	-.1784+2	-.4250+2	-.1195+3	-.3718+3	-.8279+3
s5	.1746+2	.4774+2	.1263+3	.2824+3	.4534+3

Table 6. Normal modes of $l=1$ calculated with mixed and pure scaloidal-poloidal ansatz. Polytrope 2.0

Mixed scaloidal - poloidal ansatz :

*	.2301-1	.7249-1	.2619	.5062	.5402	.8158	.1180+1	.1208+1	.2326+1	.4871+1
p1	-.3971	.1306+1	-.1314+1	.1213+1	-.8912	-.1773+1	-.1681+1	.2049+1	-.3869	.1136
p2	.1353+1	-.4312+1	.6661+1	-.8100+1	.4411+1	.1504+2	.2212+2	-.2315+2	.3658+1	-.1285+1
p3	-.2335+1	.7414+1	-.1184+2	.1413+2	-.6444+1	-.3565+2	-.8687+2	.8409+2	-.1125+2	.4585+1
p4	.2079+1	-.6651+1	.1187+2	-.7989+1	.3405+1	.2544+2	.1313+3	-.1218+3	.1400+2	-.6472+1
p5	-.7381	.2344+1	-.4998+1	.1897+1	-.1036+1	-.6703	-.6726+2	.6086+2	-.6114+1	.3142+1
s1	.4019+1	.6560	.7069	-.1378+1	-.1912+1	.4493	.2642+1	.2191+1	-.3421+1	.9344+1
s2	.1677+1	.8264	-.1765+1	.1457+1	-.1594+1	-.2904+1	-.1548+2	-.9469+1	.1835+1	-.1495+3
s3	.9296+1	.9079+1	-.1648+1	.1745+2	.3275+2	-.6920	.4603+2	.3397+2	.1940+3	.6977+3
s4	-.1897+2	-.1757+2	-.2517+1	-.3578+2	-.6651+2	.1294+2	-.1439+3	-.1577+3	-.6187+3	-.1223+4
s5	.2144+2	.2021+2	.2126+1	.3686+2	.8862+2	-.6731+1	.1549+3	.1835+3	.4897+3	.7136+3
	s	p	p	s	p	p	s	sp	s	s

Pure polidal modes :

*	.8092-1	.2757	.5223	.8245	.1201+1
p1	.1298+1	-.1351+1	.1500+1	-.1790+1	-.2688+1
p2	-.4081+1	.6487+1	-.9057+1	.1486+2	.3248+2
p3	.6857+1	-.1123+2	.1464+2	-.3413+2	-.1222+3
p4	-.6050+1	.1135+2	-.7592+1	.2255+2	.1802+3
p5	.2097+1	-.4841+1	.1800+1	.9343	-.9099+2

Pure scaloidal ansatz :

*	.2691-1	.5166	.1179+1	.2310+1	.4866+1
s1	.4049+1	-.2437+1	.3469+1	-.3458+1	.9344+1
s2	.1854+1	-.4873	-.1778+2	.2414+1	-.1496+3
s3	.1133+2	.3707+2	.5476+2	.1922+3	.6984+3
s4	-.2288+2	-.7293+2	-.2083+3	-.6178+3	-.1225+4
s5	.2588+2	.9313+2	.2368+3	.4905+3	.7147+3

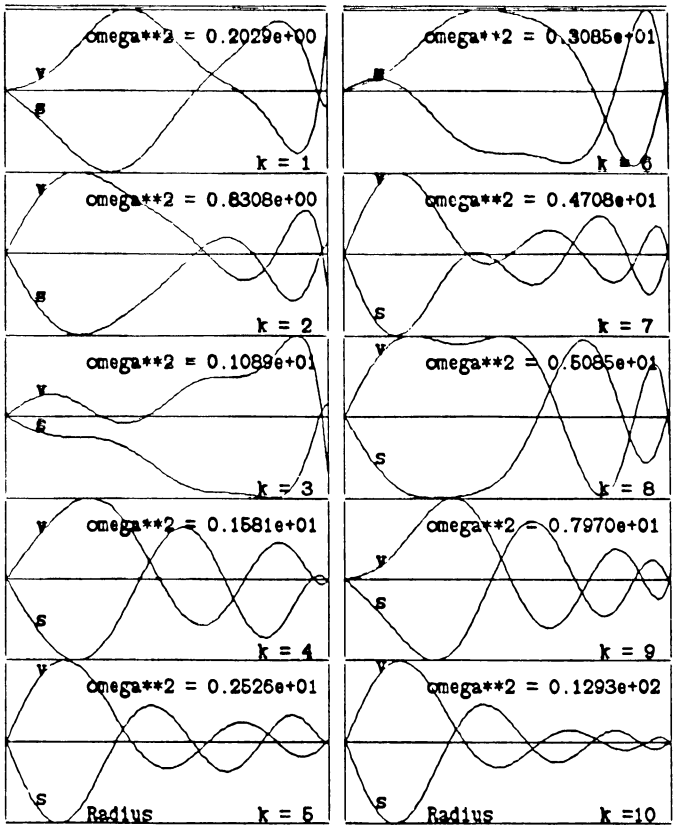

Fig. 6. Radial dependence of volume (v) and of surface (s) density waves; $n=1.0$, $l=1$

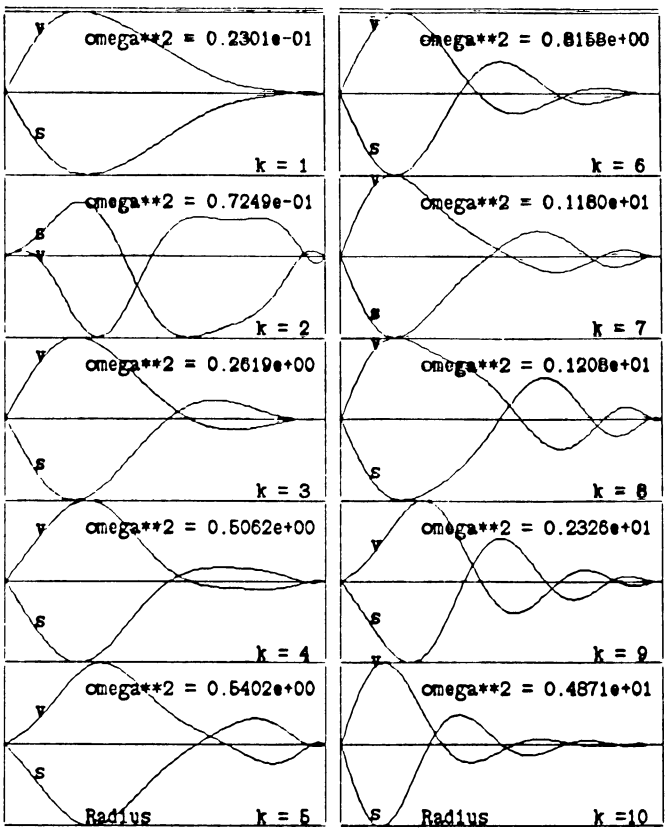

Fig. 8. Radial dependence of volume (v) and of surface (s) density waves; $n=2.0$, $l=1$

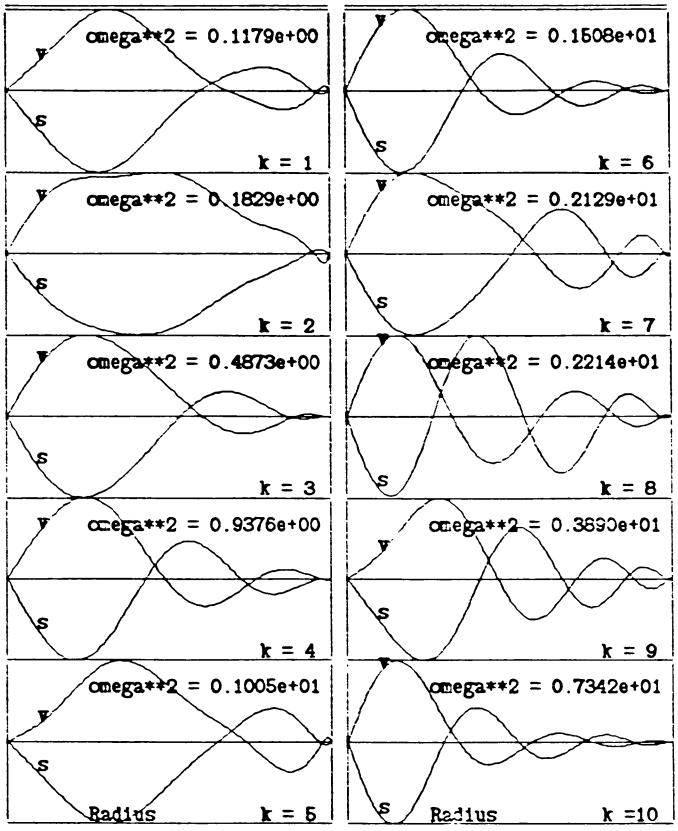

Fig. 7. Radial dependence of volume (v) and of surface (s) density waves; $n=1.5$, $l=1$

(13c), for $l=1$, $k=0$, $m=0$, gives $\zeta_{t10}=[0,0,-(\varrho/\Psi)\,r\sin\theta]$. The Lagrangian displacement corresponding to this vector is $\eta_{t10}=[0,0,(i/\omega)\,r\sin\theta]$; see Eq. (14). In the case of a fluid this is a solid-body rotation of the fluid and is neutral (i.e., it is an exact eigenfunction with zero eigenfrequency). In the stellar system case, however, there is a velocity perturbation induced by this ζ_{t10}; see Eq. (5). It is not exactly a solid body rotation. However, convergence of the lowest toroidal eigenvalue to zero indicates that it is very close to it. In polytrope 2.5, $\varrho/\Psi=1$; see Eqs. (16b) and (16c). The two vectors ζ_{t10} and η_{t10} become identical. The corresponding element of the W 1-matrix, W_{t1t1}, vanishes; see Eq. (35). Thus, the lowest toroidal eigenvalue becomes exactly zero. This feature is exclusive to $l=1$.

Finally let us observe that the toroidal modes do not induce density waves. They only give rise to a macroscopic velocity field, $\boldsymbol{u}=\dot{\boldsymbol{\eta}}=-(\Psi/\varrho)\,\boldsymbol{\xi}$; see Sect. 4.1.

We close this section by making a final comparison between the stellar system problem and the fluid one. It has been advocated throughout the paper that the Hilbert space of the eigenmodes of both systems are identical. Here we observe further features common to both problems. The counterpart of the pressure modes of a fluid are the scaloidal modes of a stellar system, and the counterpart of the gravity modes of a fluid are the poloidal modes. There are also differences. The sequence of the eigenvalues of the gravity modes starts from a highest value and converges to zero as the mode order (the number of nodes, say) increases to ∞, while that of the pressure modes starts from a lowest value and increases without bound. Convergence to zero is not observed in stellar systems. Both sequences of the scaloidal and poloidal modes start from a lowest value and increase with increasing mode orders. It appears, however, that the poloidal eigenvalues fall in general

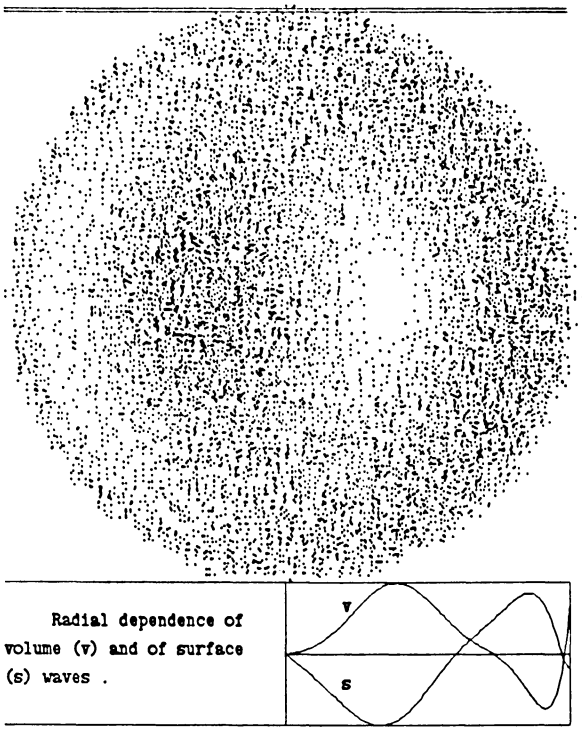

Fig. 9. A surface density wave of the polytrope $n = 1.0$; non-radial mode $l = 1$, $k = 1$, $\omega^2 = 0.2029$. The density of dots is zero at minimum mass density and is maximum at maximum mass density

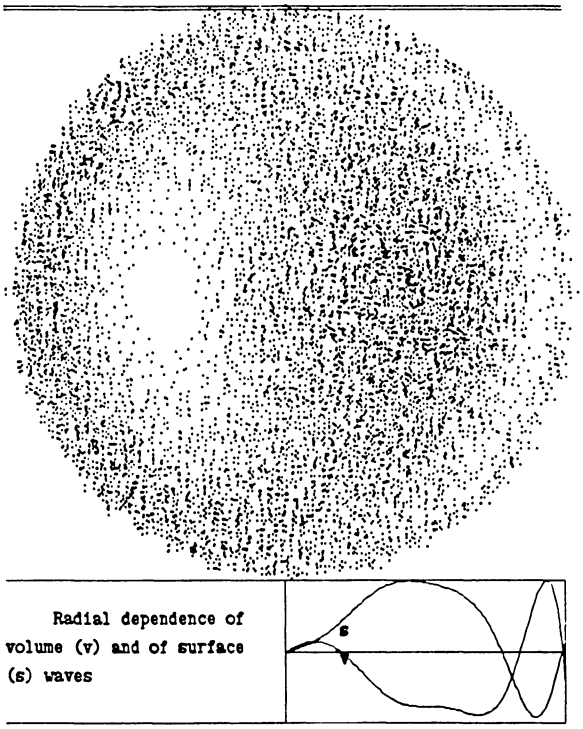

Fig. 10. A surface density wave of the polytrope $n = 1.0$; non-radial mode $l = 1$, $k = 6$, $\omega^2 = 0.3085\mathrm{E}+01$. The density of dots is zero at minimum mass density and is maximum at maximum mass density

Table 7. Eigenvalues of non-radial toroidal oscillations of polytropes

6724-1					n=1.0, l=1
.7397-3	.6672				
.1057-3	.5735	.1401+1			
.2718-4	.5545	.1290+1	.2314+1		
.9422-5	.5518	1225+1	.2201+1	.3411+1	
.1156-1					n=1.5, l=1
.4543-3	.3457				
.7480-4	.3457	.7648			
.2055-4	.3399	.7462	.1329+1		
.7447-5	.3376	.7376	.1247+1	.2046+1	
.1212-2					n=2.0, l=1
.8409-4	.2020				
.1580-4	.1865	.4801			
.4620-5	.1865	.4030	.8723		
.1738-5	.1862	.4000	.6903	.1377+1	
.0					n=2.5, l=1
.0	.1160				
.0	.9298-1	.2921			
.0	.9154-1	.2087	.5450		
.0	.9152-1	.1982	.3711	.8726	
.1907-3					n=3.0, l=1
.2142-4	.5963-1				
.4992-5	.4134-1	.1569			
.1638-5	.3942-1	.9680-1	.2995		
.6618-6	.3917-1	.8737-1	.1773	.4872	
.2425-3					n=3.5, l=1
.3077-4	.2482-1				
.7802-5	.1513-1	.6754-1			
.2693-5	.1395-1	.3657-1	.1319		
.1126-5	.1370-1	.3168-1	.6829-1	.2189	
.1218-3					n=4.0, l=1
.1698-4	.6986-2				
.4630-5	.3852-2	.1940-1			
.1673-5	.3446-2	.9477-2	.3870-1		
.7221-6	.3333-2	.7983-2	.1784-1	.6560-1	
.1983-4					n=4.5, l=1
.3027-5	.7816-3				
.8795-6	.4044-3	.2175-2			
.3315-6	.3524-3	.1001-2	.4376-2		
.1475-6	.3352-3	.8279-3	.1882-2	.7523-2	

behind the scaloidal values and increase at a slower pace than their scaloidal counterparts. One further noteworthy difference: While the toroidal modes of a fluid are neutral, those of a stellar system are not. In other words, the non-neutral modes of fluids are bispectral, pressure- and gravity-modes. Those of a stellar system are *trispectral*, scaloidal-, poloidal-, and toroidal-modes.

8.3. Comparison of wave frequencies with particle orbital frequencies

This section and the following are devoted to the question of interaction between particles and waves. Here we search out the modes whose frequencies lie outside the range of the admissible particle frequencies. There are such modes and the question of wave-particle resonance does not arise for them.

Within a spherical system of uniform density ϱ, a particle is subject to the gravitational force $-(1/3)4\pi G\varrho \boldsymbol{r}$. Its motion is a three dimensional harmonic oscillation with the angular frequency $\omega^2 = (1/3)4\pi G\varrho$. In an actual stellar system the density is sufficiently uniform in the immediate neighborhood of the center, and orbits with ω^2 as large as $(1/3)4\pi G\varrho_c$ can exist, where ϱ_c is the central density. Thus the lowest upper limit to ω^2 is $(1/3)4\pi G\varrho_c$.

Similarly a lower limit to ω^2 is $(1/3)4\pi G\bar{\varrho}$, where $\bar{\varrho}$ is the mean density of the system. An improved lower limit can, however, be obtained. Let us consider a highly centrally condensed system of

Table 8. The lower limits of $\omega^2_{\text{particle}}$ for polytropes. The unit is $4\pi G\varrho_c$. A number a $10^{\pm b}$ is written as $a\pm b$

Polytropic index	1.0	1.5	2.0	2.5	3.0	3.5	4.0	4.5
$(1/3)\bar{\varrho}/\varrho_c$	0.101	0.556–1	0.292–1	0.142–1	0.615–2	0.218–2	0.536–3	0.539–4
$(8/3)\bar{\varrho}/\varrho_c$	–	–	0.234	0.114	0.492–1	0.175–1	0.429–2	0.431–3

the total mass M and the finite radius R. Particles move in Keplerian orbits with $\omega^2 = GM/a^3$, where a is the semi major axis of the orbit. Particles reaching the outermost regions of the system have highly elliptical orbits with $a = R/2$, and have *the lowest* $\omega^2 = 8\pi GM/R^3 = (8/3)4\pi G\bar{\varrho}$. Thus, the largest lower limit lies somewhere between 1 to 8 times $(1/3)4\pi G\bar{\varrho}$.

In units of $4\pi G\varrho_c$ (the unit used for normal mode frequencies of this paper) the admissible ω^2 for particle motions falls in the range

$$\frac{\alpha}{3}\frac{\bar{\varrho}}{\varrho_c} < \omega^2 \text{ (particle)} < \frac{1}{3}, \qquad \text{where } 1 < \alpha < 8.$$

The higher the central condensation the closer α to 8. These lower limits for polytropes are given in Table 8 (the data for $\bar{\varrho}/\varrho_c$ is from Chandrasekhar, 1957).

In Table 1 many of the radial eigenvalues are larger than 1/3, the lowest upper limit for particles. Examples are all modes of polytropes 1.0 and 1.5, the second and higher modes of polytropes 2.0 and 2.5, and many higher modes of other polytropes. There are no eigenvalues smaller than the lower limits of Table 8.

In Table 3, many non-radial eigenvalues of $l=1$ are larger than 1/3. Examples are the second and higher modes of polytropes 1.0 and 1.5, the third and higher modes of polytropes 2.0 and 2.5, etc. Two of the eigenvalues are smaller than the lower limits. These are the first modes of the highly centrally condensed polytropes 4.0 and 4.5.

There is no need to compare the toroidal frequencies of Table 7 with particle frequencies. These modes do not perturb the equilibrium gravitational field and do not interact with particles.

8.4. *Particle – wave interaction*

In the earlier sections we have strictly confined ourselves to the mean-field approximation and have ignored particle individualities completely. In this section we abandon this consistency and ask what happens to a particle placed in the smoothed-out but perturbed system. Let us consider a normal mode of the type contemplated in this paper and a particle in its Keplerian orbit in the system. The equation of motion of the particle at position $\boldsymbol{r}$ is

$$\ddot{\boldsymbol{r}} = -\nabla U(r) - \nabla\delta U(\boldsymbol{r}, t), \tag{43}$$

where $U(r)$ is the unperturbed gravitational field and $\delta U(\boldsymbol{r}, t) = \delta U(\boldsymbol{r})\exp i\omega t$ is the perturbation induced by the wave. On multiplying Eq. (43) by $\boldsymbol{v} = \dot{\boldsymbol{r}}$ and integrating with respect to time from 0 to t one arrives at:

$$\frac{1}{2}v^2 + U(r) + \int_0^t \dot{\boldsymbol{r}}\cdot\nabla\delta U\,dt = \text{const}. \tag{44}$$

The total time derivative of δU is

$$\frac{d\delta U}{dt} = \frac{\partial\delta U}{\partial t} + \dot{\boldsymbol{r}}\cdot\nabla\delta U. \tag{45}$$

Substituting for the integrand in Eq. (44) from Eq. (45) one obtains

$$\begin{aligned}\int_0^t \dot{\boldsymbol{r}}\cdot\nabla\delta U\,dt &= \int_0^t\left[\frac{d\delta U}{dt} - \frac{\partial\delta U}{\partial t}\right]dt \\ &= \delta U(\boldsymbol{r}, t) - \delta U(\boldsymbol{r}_0, 0) - \delta U(\boldsymbol{r}_0, t) + \delta U(\boldsymbol{r}_0, 0) \\ &= \delta U(\boldsymbol{r}, t) - \delta U(\boldsymbol{r}_0, t).\end{aligned} \tag{46}$$

Equation (44) becomes

$$\tfrac{1}{2}v^2 + U(r) + [\delta U(\boldsymbol{r}) - \delta U(\boldsymbol{r}_0)]\,e^{i\omega t} = \text{const}. \tag{47}$$

As expected, the total energy of the particle, $\frac{1}{2}v^2 + U(r) + \delta U(\boldsymbol{r}, t)$ is not constant in time and there is a transfer of energy from the wave to the particle, but also from the particle to the wave, if the expression in the square bracket is negative. This is not surprising. The wave-particle combination is a Hamiltonian system subject to time reversibility. During one complete period of motion some energy exchange will take place, but whatever happens in half the period will be undone in the following half. Indeed, Eq. (47) clearly shows that if $\boldsymbol{r}$ and $\boldsymbol{r}_0$ happen to lie on the same equipotential of $\delta U(\boldsymbol{r})$, the energy of the particle returns to its unperturbed value $\frac{1}{2}v^2 + U(\boldsymbol{r}) = \text{const}$. The wave is not damped, nor the particle absorbs unlimited quantities of energy from the mode on account of resonance.

In addition to this argument there are other considerations. i) The toroidal modes of any spherical system belonging to $m = 0$ and ± 1 do not induce perturbations in the density or in the gravitational potential. There is no coupling between particle orbits and the waves. ii) The polytrope 1.5 has the distribution function $F(E) = \text{const.}$ and $dF/dE = 0$. Perturbation in the total gravitational energy for all modes is identically zero (this is the same as vanishing of the W 2-integral for this polytrope; see Eq. [I.45]). Therefore, to begin with there is no potential energy in the wave to be trensferred to the particle, iii) Finally let us quote Miller's point of view. A harmonic oscillator with a constant frequency can resonate in a time varying force field which has the same frequency. A mass point in a Kepler orbit in a gravitational field, however, has an orbit dependent frequency. If the time varying field moves the particle from one orbit to the other, the orbital frequency will also change and the conditions for resonance will be destroyed.

Acknowledgement. I wish to thank Professor S. Chandrasekhar for advice on terminology and notation, and for his encouragement. I am grateful to Professor P. O. Vandervoort and Professor R. H. Miller for valuable discussions. The work was completed while the author was on leave from Shiraz University, Department of Physics, at the University of Chicago, Astronomy and Astrophysics Center. Financial help and hospitalities of both institutions, as well as a travel grant from the International Astronomical Union, are greatly appreciated. The work has received partial support from the NSF grant Nr. AST 82-18385 with the University of Chicago, and the Research Council of Shiraz University.

Note added in March 1986

In the course of refereeing this paper a dialog was exchanged between the referee (Frank H. Shu) and the author. A good deal of the differences of opinions were reconciled. There, however, remains a reservation which the referee recommends to bring to the attention of the readers. This is duly done by including a summary of the relevant points of the dialog below.

Referee: ... the Hilbert space methods that Sobouti introduces to do the configuration space analysis are quite powerful; unfortunately, an approximation of dubious accuracy is adopted right at the outset, the assumption that the antisymmetric part of the perturbation in the distribution function is linear in the velocity $\boldsymbol{v}$ (see Eq. [5]). For a general choice of the equilibrium distribution function, $F(E)$, this form does not satisfy the fundamental Eq. (1b); thus, the subsequent analysis for the eigenvalue problem resulting from Eq. (3) contains an uncontrolled approximation whose errors are independent of the accuracy or completeness of the trial functions constructed for ξ. This defect would not be fatal if the author could give a plausible physical argument which justifies why Eq. (5), a drastic truncation of a power series expansion which may itself have limited convergence properties (at large $|\boldsymbol{v}|$), represents a reasonable ansatz. Alternatively, the author should give a mathematical demonstration which shows that its adoption does not seriously affect the numerical results.

Author: ... Eq. (5) is the first term of an absolutely convergent series and is used as a variational ansatz. No variational ansatz is expected to satisfy the differential equation of motion to which it pertains. Yet the second order accuracy of the calculated eigenvalues is guaranteed by the variational principle. ...

After revision:

Referee: .... An assumed linear dependence on $\boldsymbol{v}$ suffers the opposite criticism (from an assumed linear dependence in $\boldsymbol{x}$) since one intuitively expects stars of high random velocity to partake less than stars of low random velocity in any coherent oscillations of the system. This is certainly the case in density-wave theory. Dr. Sobouti has alleviated part of my worry by pointing out the truncation at the escape velocity, but I am still concerned that the basic ansatz assumes a *qualitatively* wrong assumption, namely that f increases with increasing $\boldsymbol{v}$. I worry that this assumption underlies the finding that the eigenfrequencies are generally larger than the characteristic orbital frequencies of the system. If they are not, then *resonances* can arise and the discussion on pp. 108–109 is invalidated. ...

Author: In a forthcoming paper we attempt to include third order-in-velocity terms in the variational ansatz of Eq. (5). Let us hope that the new computations will throw some light on the issue and provide something more than intuitive feelings to base the judgement on.

References

Chandrasekhar, S.: 1961, Hydrodynamic and Hydromagnetic Stability, Oxford, Clarendon Press, p. 6.622

Chandrasekhar, S.: 1957, Stellar Structure, New York, Dover Publication, p. 155

Cox, J.P., Giuli, R.T.: 1968, Principles of Stellar Structure, New York, Gordon and Breech, Vol. **2**, p. 1051

Dixit, V.V., Sarath, B., Sobouti, Y.: 1980, *Astron. Astrophys.* **89**, 259

Elsasser, W.M.: 1946, *Phys. Rev.* **69**, 106

Hurley, M., Roberts, P.H., Wright, K.: 1966, *Astrophys. J.* **143**, 535

Kalnajs, A.J.: 1977, *Astrophys. J.* **212**, 637

King, I.R.: 1967, Dynamics of Star Clusters, in *Relativity Theory and Astrophysics* **2**, *Galactic Structures*, ed. J. Ehlers, Am. Math. Soc., p. 116

Kulsrud, R.M., Mark, J.W.-K.: 1971, *Astrophys. J.* **160**, 471

Ledoux, P., Walraven, Th.: 1958, Handbuch der Physik **51**, p. 353

Miller, R.H.: 1985, (private communication)

Sobouti, Y.: 1977, *Astron. Astrophys.* **55**, 327

Sobouti, Y.: 1980, *Astron. Astrophys.* **89**, 314

Sobouti, Y.: 1981, *Astron. Astrophys.* **100**, 319

Sobouti, Y.: 1984, *Astron. Astrophys.* **140**, 82 (Paper I)

Sobouti, Y.: 1985, *Astron. Astrophys.* **147**, 61 (Paper II)

Toomre, A.: 1977, *Ann. Rev. Astron. Astrophys.* **15**, 437

Vandervoot, P.O.: 1983, *Astrophys. J.* **273**, 511